

## Loss of *Dnmt3a* increased self-renewal and resistance to pegIFN $\alpha$ in *JAK2-V617F*-positive myeloproliferative neoplasms

Tracking no: BLD-2023-020270R2

Marc Usart (University Hospital Basel and University of Basel, Switzerland) Jan Stetka (University Hospital Basel and University of Basel, Switzerland, Switzerland) Damien Luque Paz (Univ Angers, Nantes Université, CHU Angers, Inserm, CNRS, CRI2NA, F-49000, Angers, France, France) Nils Hansen (University Hospital of Basel, Switzerland) Quentin Kimmerlin (University Hospital Basel and University of Basel, Switzerland) Tiago Almeida Fonseca (University Hospital Basel and University of Basel, Switzerland) Melissa Lock (University Hospital Basel and University of Basel, Switzerland, Switzerland) Lucia Kubovcakova (University Hospital Basel and University of Basel, Switzerland) Riikka Karjalainen (University Hospital Basel and University of Basel, Switzerland, Switzerland) Hui Hao-Shen (Swiss Institute of Bioinformatics, Basel, Switzerland, Switzerland) Anastasiya Börsch (Swiss Institute of Bioinformatics, Basel, Switzerland, Switzerland) Athimed El Taher (University Hospital Basel and University of Basel, Switzerland) Jessica Schulz (ETH Zurich, Switzerland) Jean-Christophe Leroux (ETH Zurich, Switzerland) Stefan Dirnhofer (UNIVERSITY HOSPITAL BASEL, Switzerland) Radek Skoda (University Hospital Basel and University of Basel, Switzerland)

### Abstract:

Pegylated interferon alpha (pegIFN $\alpha$ ) can induce molecular remissions in *JAK2-V617F*-positive myeloproliferative neoplasms (MPN) patients by targeting long-term hematopoietic stem cells (LT-HSCs). Additional somatic mutations in genes regulating LT-HSC self-renewal, such as *DNMT3A*, have been reported to have poorer responses to pegIFN $\alpha$ . We investigated if *DNMT3A* loss leads to alterations in *JAK2-V617F* LT-HSCs functions conferring resistance to pegIFN $\alpha$  treatment in a mouse model of MPN and in hematopoietic progenitors from MPN patients. Long-term treatment with pegIFN $\alpha$  normalized blood parameters, reduced splenomegaly and *JAK2-V617F*-chimerism in single-mutant *JAK2-V617F* (VF) mice. However, pegIFN $\alpha$  in VF;*Dnmt3a* $\Delta/\Delta$  (VF;*Dm* $\Delta/\Delta$ ) mice worsened splenomegaly and failed to reduce *JAK2-V617F*-chimerism. Furthermore, LT-HSCs from VF;*Dm* $\Delta/\Delta$  mice compared to VF were less prone to accumulate DNA damage and exit dormancy upon pegIFN $\alpha$  treatment. RNA-sequencing showed that IFN $\alpha$  induced stronger upregulation of inflammatory pathways in LT-HSCs from VF;*Dm* $\Delta/\Delta$  compared to VF mice, indicating that the resistance of VF;*Dm* $\Delta/\Delta$  LT-HSC was not due to failure in IFN $\alpha$  signaling. Transplantations of bone marrow from pegIFN $\alpha$  treated VF;*Dm* $\Delta/\Delta$  mice gave rise to more aggressive disease in secondary and tertiary recipients. Liquid cultures of hematopoietic progenitors from MPN patients with *JAK2-V617F* and *DNMT3A* mutation showed increased percentages of *JAK2-V617F*-positive colonies upon IFN $\alpha$  exposure, whereas in patients with *JAK2-V617F* alone the percentages of *JAK2-V617F*-positive colonies decreased or remained unchanged. PegIFN $\alpha$  combined with 5-azacytidine only partially overcame resistance in VF;*Dm* $\Delta/\Delta$  mice. However, this combination strongly decreased the *JAK2*-mutant allele burden in mice carrying VF mutation only, showing potential to inflict substantial damage preferentially to the *JAK2*-mutant clone.

**Conflict of interest:** COI declared - see note

**COI notes:** R.C.S. is a scientific advisor/SAB member and has equity in Ajax Therapeutics, he consulted for and/or received honoraria from Novartis, BMS/Celgene, AOP, GSK, Baxalta and Pfizer. N.H. owns stocks in the company Cantargia. The remaining authors declare no competing financial interests.

**Preprint server:** No;

**Author contributions and disclosures:** MU and JS designed and performed research, analyzed data and wrote the manuscript, DLP, NH, QK, TAF, ML, LK, RK and HHS, performed research and analyzed data, AB, AT, JS, JCL and SD analyzed data, RCS designed research, analyzed data and wrote the manuscript.

**Non-author contributions and disclosures:** No;

**Agreement to Share Publication-Related Data and Data Sharing Statement:** RNAseq raw and processed data are available on the Gene Expression Omnibus with accession numbers GSE225918 (scRNAseq) and GSE255253 (bulk RNAseq)

**Clinical trial registration information (if any):**

## Loss of *Dnmt3a* increased self-renewal and resistance to pegIFN $\alpha$ in *JAK2-V617F*-positive myeloproliferative neoplasms

Marc Usart<sup>1\*</sup>, Jan Stetka<sup>1,2\*</sup>, Damien Luque Paz<sup>3</sup>, Nils Hansen<sup>1</sup>, Quentin Kimmerlin<sup>1</sup>, Tiago Almeida Fonseca<sup>1</sup>, Melissa Lock<sup>1</sup>, Lucia Kubovcakova<sup>1</sup>, Riikka Karjalainen<sup>1</sup>, Hui Hao-Shen<sup>1</sup>, Anastasiya Börsch<sup>4,5</sup>, Athimed El Taher<sup>4,5</sup>, Jessica Schulz<sup>6</sup>, Jean-Christophe Leroux<sup>6</sup>, Stefan Dirnhofer<sup>7</sup>, and Radek C. Skoda<sup>1</sup>

\* Contributed equally

<sup>1</sup>Department of Biomedicine, Experimental Hematology, University Hospital Basel and University of Basel, Basel, Switzerland.

<sup>2</sup>Department of Biology, Faculty of Medicine and Dentistry, Palacky University, Olomouc, Czech Republic.

<sup>3</sup>Univ Angers, Nantes Université, CHU Angers, Inserm, CNRS, CRCI2NA, F-49000, Angers, France.

<sup>4</sup>Department of Biomedicine, Bioinformatics, University of Basel and University Hospital Basel, Basel, Switzerland.

<sup>5</sup>Swiss Institute of Bioinformatics, Basel, Switzerland.

<sup>6</sup>Institute of Pharmaceutical Sciences, ETH Zurich, Zurich, Switzerland.

<sup>7</sup>Institute of Medical Genetics and Pathology, University Hospital Basel, Basel, Switzerland.

**Key words:** myeloproliferative neoplasms, interferon- $\alpha$ , *Dnmt3a*, *JAK2-V617F*

**Running Title:** Loss of *Dnmt3a* confers resistance to pegIFN $\alpha$

### Statement of prior presentation

Oral Presentation at the 62<sup>nd</sup> Annual meeting of the American Society of Hematology, San Diego, CA, 7 December 2020.

**Article type:** Regular Article

**Scientific Category:** Myeloid Neoplasia

**Word count:** Abstract: 248  
Text: 4272

**Figure count:** 7

**References** 50

**Corresponding author:** radek.skoda@unibas.ch

Department of Biomedicine, Experimental Hematology, University Hospital Basel and University of Basel, Hebelstrasse 20, 4031Basel, Switzerland.

### Data Sharing Statement

Additional methods are described and available with the online version of this article. For original data and reagents, please contact [radek.skoda@unibas.ch](mailto:radek.skoda@unibas.ch).

RNAseq raw and processed data are available on the Gene Expression Omnibus with accession numbers GSE225918 (scRNAseq) and GSE255253 (bulk RNAseq)

### Key points

- Loss of *Dnmt3a* increases self-renewal of *JAK2-V617F* hematopoietic stem cells and mitigates their attrition upon chronic pegIFN $\alpha$  treatment
- A combination of pegIFN $\alpha$  and 5-azacytidine can strongly decrease the *JAK2*-mutant allele burden in MPN driven by *JAK2-V617F* alone

### Explanation of Novelty (497 of 500 characters with spaces max.)

Patients with mutations in *JAK2-V617F* and *Dnmt3a* (*VF;Dm<sup>Δ/Δ</sup>*) are known to be resistant to pegIFN $\alpha$ . We show that mouse and human hematopoietic stem cells (HSCs) are protected from the effects of IFN $\alpha$  by increased self-renewal and stemness mediated

by the loss of *Dnmt3a*. PegIFN $\alpha$  combined with 5-azacytidine partially overcomes resistance in *VF;Dm <sup>$\Delta\Delta$</sup>*  mice, and strongly decreases the *JAK2*-mutant allele burden in single mutant *VF* mice, showing potential to substantially reduce the *JAK2*-mutant clone.

## Abstract

Pegylated interferon alpha (pegIFN $\alpha$ ) can induce molecular remissions in *JAK2*-V617F-positive myeloproliferative neoplasms (MPN) patients by targeting long-term hematopoietic stem cells (LT-HSCs). Additional somatic mutations in genes regulating LT-HSC self-renewal, such as *DNMT3A*, have been reported to have poorer responses to pegIFN $\alpha$ . We investigated if *DNMT3A* loss leads to alterations in *JAK2*-V617F LT-HSCs functions conferring resistance to pegIFN $\alpha$  treatment in a mouse model of MPN and in hematopoietic progenitors from MPN patients. Long-term treatment with pegIFN $\alpha$  normalized blood parameters, reduced splenomegaly and *JAK2*-V617F-chimerism in single-mutant *JAK2*-V617F (*VF*) mice. However, pegIFN $\alpha$  in *VF;Dnmt3a $\Delta\Delta$*  (*VF;Dm $\Delta\Delta$* ) mice worsened splenomegaly and failed to reduce *JAK2*-V617F-chimerism. Furthermore, LT-HSCs from *VF;Dm $\Delta\Delta$*  mice compared to *VF* were less prone to accumulate DNA damage and exit dormancy upon pegIFN $\alpha$  treatment. RNA-sequencing showed that IFN $\alpha$  induced stronger upregulation of inflammatory pathways in LT-HSCs from *VF;Dm $\Delta\Delta$*  compared to *VF* mice, indicating that the resistance of *VF;Dm $\Delta\Delta$*  LT-HSC was not due to failure in IFN $\alpha$  signaling. Transplantations of bone marrow from pegIFN $\alpha$  treated *VF;Dm $\Delta\Delta$*  mice gave rise to more aggressive disease in secondary and tertiary recipients. Liquid cultures of hematopoietic progenitors from MPN patients with *JAK2*-V617F and *DNMT3A* mutation showed increased percentages of *JAK2*-V617F-positive colonies upon IFN $\alpha$  exposure, whereas in patients with *JAK2*-V617F alone the percentages of *JAK2*-V617F-positive colonies decreased or remained unchanged. PegIFN $\alpha$  combined with 5-azacytidine only partially overcame resistance in *VF;Dm $\Delta\Delta$*  mice. However, this combination strongly decreased the *JAK2*-mutant allele burden in mice carrying *VF* mutation only, showing potential to inflict substantial damage preferentially to the *JAK2*-mutant clone.

## Introduction

*JAK2-V617F* alone or together with additional somatic mutations is found in the majority of patients with MPN.<sup>1</sup> The presence of additional mutations correlates with worse outcome,<sup>2,3</sup> and "high molecular risk" (HMR) mutations with a strong negative impact on outcome have been identified.<sup>4</sup> Although mutations in *DNMT3A* are relatively frequent in MPN patients (~5-6%),<sup>5</sup> and their frequencies are increased in MPN patients that progress to AML (~16%),<sup>6</sup> it remains controversial whether they should also be considered as HMR. *DNMT3A* is the most frequently mutated gene in individuals with clonal hematopoiesis of indetermined potential (CHIP),<sup>7-9</sup> and CHIP is associated with increased risk for hematological malignancies.<sup>10-12</sup> *DNMT3A* mutations frequently occur in the methyltransferase domain around residue R882, resulting in loss of activity with dominant-negative effect over wild-type *DNMT3A*.<sup>13</sup> *DNMT3A* mutations lead to focal hypomethylation and loss of epigenetic silencing of self-renewal genes in long-term hematopoietic stem cells (LT-HSC),<sup>14</sup> thereby increasing stemness and self-renewal of LT-HSC.<sup>15-17</sup> MPN patients responded to interferon-alpha ( $\text{IFN}\alpha$ ) in some cases with a substantial reduction in *JAK2-V617F* allelic burden.<sup>18,19</sup> In mouse models of MPN,  $\text{IFN}\alpha$  preferentially targets *Jak2-V617F* mutant LT-HSCs,<sup>20,21</sup> involving mechanisms of cell cycle activation, reactive oxygen species (ROS) induction and accumulation of DNA damage.<sup>22</sup> Here we examined how loss of *Dnmt3a* protects the *JAK2*-mutant clone from the effects of  $\text{IFN}\alpha$  in a *JAK2-V617F* mouse model and in primary hematopoietic cells from patients with MPN.

## Materials and Methods

### Mice

Conditional *JAK2-V617F* transgenic "flip-flop" (*FF*) mice,<sup>23</sup> *Dnmt3a* floxed knockout mice,<sup>24</sup> and *UBC-GFP* reporter mice,<sup>25</sup> were intercrossed with tamoxifen-inducible *SclCre<sup>ER</sup>* mice.<sup>26</sup> *Cre<sup>ER</sup>* enzymatic activity was induced by intraperitoneal injection of 2 mg tamoxifen (Sigma Aldrich) for 5 consecutive days, repeated for 4 consecutive weeks. All mice used in this study had pure C57BL/6N background and were maintained under specific pathogen-free conditions in accordance with Swiss federal regulations. All animal experiments were approved by the Cantonal Veterinary Office of Basel-Stadt, Switzerland.

### Production of pegylated mouse interferon- $\alpha$

Mouse IFN $\alpha$  was purified from culture supernatants of the NS0 mouse myeloma cell line stably transfected with a cDNA encoding mouse IFN $\alpha$ 4.<sup>27</sup> The cells were switched to serum-free media and supernatants were collected after 5 days. Details are provided in Supplemental Methods.

### MPN patients

Blood samples from MPN patients collected (Supplemental Table 1), and diagnosis was established according to the World Health Organization criteria.<sup>28</sup> The study was approved by the local Ethics Committees (Ethik Kommission Beider Basel) and written informed consent was obtained from all patients in accordance with the Declaration of Helsinki. The culture of CD34<sup>+</sup> cells from peripheral blood of MPN patients and assessment of responses to IFN $\alpha$  are described in detail in the Supplemental Methods.

Blood samples and clinical data of MPN patients were collected at the University Hospital Basel, Switzerland. The study was approved by the local Ethics Committees (Ethik Kommission Beider Basel). Written informed consent was obtained from all patients in accordance with the Declaration of Helsinki.



## Results

### Phenotypic characterization of *VF* and *VF;Dm<sup>Δ/Δ</sup>* mice

We compared the phenotypes of *ScfCre;FF1* (*VF*) mice with *ScfCre;FF1;Dnmt3a<sup>Δ/Δ</sup>* (*VF;Dm<sup>Δ/Δ</sup>*) mice after tamoxifen induction (Figure 1). The efficiency of Cre-mediated deletion of the conditional *Dnmt3a<sup>fl/fl</sup>* alleles was determined by qPCR (Figure 1B; Supplemental Figure S1). *VF* mice developed PV phenotype with increased blood counts and hypoglycemia, whereas *VF;Dm<sup>Δ/Δ</sup>* mice displayed a reduction in red cell parameters and platelet counts combined with a normalization of white blood cell counts and blood glucose (Figure 1C and D). Blood counts and glucose levels were unchanged in *Dm<sup>Δ/Δ</sup>* mice compared to wildtype (*WT*) mice. Splenomegaly at 16 weeks was more pronounced in *VF* mice than in *VF;Dm<sup>Δ/Δ</sup>* mice, while spleen weight remained normal in *Dm<sup>Δ/Δ</sup>* mice (Figure 1E). Bone marrow (BM) cellularity was decreased in *VF;Dm<sup>Δ/Δ</sup>* compared to *WT* mice (Figure 1F). An increase in LT-HSCs and early progenitors was noted in BM and spleen of *VF* and *VF;Dm<sup>Δ/Δ</sup>* mice, with most pronounced increase in spleen of *VF;Dm<sup>Δ/Δ</sup>* mice (Figure 1G). Ter119-positive erythroid cells were decreased in BM, but increased in spleen of *VF* and *VF;Dm<sup>Δ/Δ</sup>* mice, mainly reflecting alterations in erythroid subpopulations III and IV (Figure 1H). At 16 weeks, *VF* mice displayed slightly higher grades of reticulin fibrosis than *VF;Dm<sup>Δ/Δ</sup>* mice (Figure 1I). *VF* mice heterozygous for the *Dnmt3a* mutation (*VF;Dm<sup>Δ/+</sup>*) showed blood counts similar to *VF;Dm<sup>Δ/Δ</sup>* mice (Supplemental Figure S2), indicating that complete loss of *Dnmt3a* is not necessary to alter the *VF* phenotype.

### Responsiveness of *VF* and *VF;Dm<sup>Δ/Δ</sup>* hematopoiesis to IFN $\alpha$

To study the effects of IFN $\alpha$  on MPN in *VF* and *VF;Dm<sup>Δ/Δ</sup>* mice we produced pegylated IFN $\alpha$  (pegIFN $\alpha$ ) from a cell line stably transfected with a cDNA encoding mouse *IFN $\alpha$ 4*.<sup>27</sup> The purified IFN $\alpha$ 4 protein was pegylated to facilitate long-term treatment of mice (Supplemental Figure S3). A pilot study was performed to determine the best pegIFN $\alpha$  dosing and setup of the competitive BM transplantation (Supplemental Figure S4). The initial pegIFN $\alpha$  dose of 100  $\mu$ g/kg\*week had to be reduced after 6 weeks, and the two maintenance doses (25  $\mu$ g/kg and 50  $\mu$ g/kg\*week) yielded similar results after

additional 12 weeks of treatment. The decrease of GFP-chimerism in the 1:1 competitive transplantation was less pronounced compared to 1:20 or 1:100 transplantations and we selected the 1:20 ratio and 25  $\mu\text{g}/\text{kg}\cdot\text{week}$  pegIFN $\alpha$  s.c. for further studies. The time-course of IFN $\alpha$  concentration in plasma after a single injection is shown in Supplemental Figure S3D. Treatment with pegIFN $\alpha$  for 16 weeks was well tolerated, normalized blood counts and decreased GFP-chimerism in most peripheral blood lineages of both *VF* and *VF;Dm $\Delta/\Delta$*  mice (Figure 2 and Supplemental Figure S5A). Spleen weight was reduced by pegIFN $\alpha$  in recipients of *VF* BM, but showed a trend towards higher values in double mutant *VF;Dm $\Delta/\Delta$*  mice compared to vehicle controls (Figure 2D).

In BM of *VF* mice, pegIFN $\alpha$  increased the frequencies of LT-HSCs and multipotent progenitors (MPPs) by increasing the numbers and percentages of GFP-negative (*WT*) cells, while decreasing GFP-positive (*JAK2*-mutant) cells in all progenitor compartments (Figure 2E). In spleen of *VF* mice, the overall frequencies of HSPCs were lower, but the same responses to pegIFN $\alpha$  were observed (Figure 2F). In *VF;Dm $\Delta/\Delta$*  mice, the overall frequencies of HSPCs decreased upon pegIFN $\alpha$  treatment, but no significant decrease in the percentages of GFP-positive (*JAK2*-mutant) cells was noted. The same behavior was observed in erythroid precursors (Supplemental Figure S5C). The proportion of CD41<sup>hi</sup> versus CD41<sup>lo</sup> subsets of LT-HSCs within the GFP-positive (*JAK2*-mutant) cells increased in *VF* transplanted mice, as previously reported.<sup>29</sup> *VF;Dm $\Delta/\Delta$*  mice showed increased proportion of CD41<sup>hi</sup> LT-HSCs already at baseline, but no increase upon pegIFN $\alpha$  treatment (Figure 2G), correlating with the resistance of the double mutant HSCs to IFN $\alpha$ . Treatment with pegIFN $\alpha$  normalized the histopathology of BM and spleen of *VF* recipients and reduced myelofibrosis and osteosclerosis, whereas *VF;Dm $\Delta/\Delta$*  double mutant mice were largely resistant to these beneficial effects of pegIFN $\alpha$  (Supplemental Figure S6).

### ***VF* and *VF;Dm $\Delta/\Delta$* mice showed differences in the accumulation of DNA damage and ROS in response to pegIFN $\alpha$**

PegIFN $\alpha$  was previously shown to preferentially affect *JAK2*-V617F mutant HSCs by inducing accumulation of DNA damage during replicative stress.<sup>22</sup> Double-stranded DNA

breaks trigger rapid phosphorylation of Ser139 on histone H2AX by PI3K-like kinases, including ATM, ATR, and DNA-PK, as an early step in the DNA damage response.<sup>30</sup> Phosphorylated H2AX ( $\gamma$ H2AX) can be detected by phospho-specific antibodies to quantify DNA damage. We found that pegIFN $\alpha$  induced phosphorylation of H2AX on Ser139, in GFP-positive  $lin^{-}/Sca1^{+}/Kit^{+}$  (LSK) cells of *VF* recipient mice, but was largely unable to do so in GFP-positive LSKs from *VF;Dm $\Delta/\Delta$*  recipients (Figure 3A). PegIFN $\alpha$  also increased the production of ROS in LSK cells from *VF* mice (Figure 3A), and to a lesser extent also in LSK cells from *VF;Dm $\Delta/\Delta$*  mice. Similar results were also obtained in LT-HSCs (Figure 3C). ROS was previously reported to induce functional attrition of HSCs in *WT* mice.<sup>31,32</sup> In GFP-positive LT-HSCs from *VF* mice, treatment with pegIFN $\alpha$  induced exit from quiescence, monitored by the marker Ki67, and an increase in DNA damage within Ki67-positive LT-HSC, monitored by the marker  $\gamma$ H2AX. In contrast, GFP-positive LT-HSCs from double-mutant *VF;Dm $\Delta/\Delta$*  mice showed no increase in cell cycle entry or DNA damage (Figure 3B). These data show that *JAK2*-mutant LT-HSCs from *VF;Dm $\Delta/\Delta$*  mice were protected against pegIFN $\alpha$  induced loss of quiescence, increased DNA damage, and ROS production.

### Functional analysis of the stem cell and progenitor compartment

To assess the effects of pegIFN $\alpha$  treatment on the functional fitness of LT-HSCs we performed secondary and tertiary transplantations (Figure 4 and Supplemental Figures S7, S8 and S9). As donors, we pooled BM cells from 3 primary recipients from the pegIFN $\alpha$  or from 3 vehicle treated recipients (Supplemental Figure S7). Using these BM cells we performed competitive and non-competitive transplantations into secondary recipients (Figure 4 and Supplemental Figure S8). In transplantations without competitor cells (Figure 4A-E), engraftment, defined as >1% GFP-chimerism in Gr1<sup>+</sup> cells in peripheral blood, was observed in all recipients. Spleen weights at 20 weeks were higher in recipients of BM from *VF;Dm $\Delta/\Delta$*  double mutant mice compared to recipients of *VF* BM, but no differences were noted between the treatment groups (Figure 4C). Secondary recipients of BM from pegIFN $\alpha$  treated *VF* donors displayed lower hemoglobin values and lower GFP-chimerism in platelets as well as decreased frequencies of GFP-positive (*JAK2*-mutant) LT-HSCs in BM than recipients of BM from vehicle-treated *VF* donors (Figure 4D and E). In contrast,

secondary recipients of BM from double mutant  $VF;Dm^{\Delta/\Delta}$  mice treated with pegIFN $\alpha$  displayed higher platelet counts than recipients of vehicle treated  $VF;Dm^{\Delta/\Delta}$  BM and GFP-chimerism was very high in all peripheral blood lineages (Figure 4D). The frequencies of LT-HSCs in BM of pegIFN $\alpha$  treated  $VF;Dm^{\Delta/\Delta}$  mice were greatly increased and consisted exclusively of GFP-positive LT-HSCs (Figure 4E).

In competitive transplantations at 1:50 ratio (Figure 4F), only about 50% of recipients of  $VF$  BM showed engraftment (>1% GFP-chimerism in peripheral blood of Gr1<sup>+</sup> cells) and none of the recipients of vehicle treated or pegIFN $\alpha$  treated BM developed MPN phenotype (Figure 4H-I). Nevertheless, pegIFN $\alpha$  treated recipients showed a trend towards lower GFP-chimerism in peripheral blood. In contrast, secondary recipients of BM from double mutant  $VF;Dm^{\Delta/\Delta}$  donor mice treated with pegIFN $\alpha$  all showed engraftment and displayed increased spleen weight than the vehicle treated group (Figure 4H), as well as higher platelet counts and higher chimerism in CD61, Gr1 and CD11b-positive peripheral blood cells (Figure 4I). The frequencies of phenotypic LT-HSCs in recipients of  $VF;Dm^{\Delta/\Delta}$  BM were expanded about 10-fold and composed almost exclusively of GFP-positive cells, whereas LT-HSCs in recipients of  $VF$  BM were almost exclusively GFP-negative and pegIFN $\alpha$  treatment had no effect (Figure 4J).

Competitive transplantations into secondary recipients at 1:250 dilutions showed the same trend towards faster rise of the GFP-chimerism in recipients of BM from pegIFN $\alpha$  treated donors (Supplemental Figure S8), but the differences to vehicle treated donors were smaller compared with the 1:50 transplantations. We calculated the frequencies of functional LT-HSCs from the competitive transplantation experiments at different dilutions using the ELDA method.<sup>33</sup>  $VF;Dm^{\Delta/\Delta}$  mice displayed approximately 10 times higher frequencies of functional LT-HSCs compared to  $VF$  mice and no differences between IFN $\alpha$  treated mice versus vehicle were observed (Supplemental Figure S8E). Thus, competitive transplantations at 1:250 with 8'000 BM cells from  $VF$  donors were limiting, but 8'000 BM cells from  $VF;Dm^{\Delta/\Delta}$  donors still contained ~8 LT-HSCs per transplant.

We also transplanted BM into tertiary recipients (Supplemental Figure S9A) and found that fewer recipients showed engraftment when pegIFN $\alpha$  treated BM cells from *VF* mice were used compared to vehicle treated *VF* BM (Supplemental Figure S9B). Recipients of *VF* BM that engrafted were unable to sustain long-term GFP-chimerism and to develop MPN phenotype (Supplemental Figure S9C). In contrast, all recipients of *VF;Dm $\Delta/\Delta$*  BM cells showed engraftment and displayed MPN phenotype with high GFP-chimerism in peripheral blood and in BM LT-HSCs (Supplemental Figure S9B-E). Again, when pegIFN $\alpha$  treated BM cells from *VF;Dm $\Delta/\Delta$*  mice were used compared to vehicle treated BM, the tertiary recipients showed higher platelet, neutrophil and monocyte counts and developed anemia.

Together, these results illustrate the increased competitiveness of double mutant *VF;Dm $\Delta/\Delta$*  BM compared to *VF* BM in secondary and tertiary transplantations and the reversal of the inhibitory effects of pegIFN $\alpha$  on *VF* BM cells into stimulatory effects on *VF;Dm $\Delta/\Delta$*  BM cells.

### **Effects of IFN $\alpha$ treatment on human progenitor and stem cells from MPN patients carrying mutations in *JAK2-V617F* and *DNMT3A* in vitro.**

To assess the effects of IFN $\alpha$  on human hematopoietic cells carrying *JAK2-V617F* alone or in combination with mutations in *DNMT3A*, we performed single cell liquid cultures of CD34+/Lin- peripheral blood cells from MPN patients and exposed them to human IFN $\alpha$  or vehicle during 10 days of culture (Figure 5A). Material from four patients that carried both *JAK2-V617F* and *DNMT3A* mutations in the same clone was available (Supplemental Figure S10). In three of these patients no other gene mutation was detectable using a targeted NGS panel covering 86 genes,<sup>2</sup> whereas one patient (P434) had an additional *TET2* mutation (Supplemental Figure S10). In all four patients the *DNMT3A* mutation preceded the acquisition of *JAK2-V617F*. As a control, we selected 4 patients that carried solely the *JAK2-V617F* mutation and were matched for age, disease subtype and *JAK2-V617F* allele burden in granulocytes from peripheral blood (Supplemental Figure S10). Growth efficiency, defined as the percentage of wells that yielded colonies, was in the range of 70% for all conditions tested (Figure 5B). The percentages of *JAK2-V617F* positive colonies increased upon IFN $\alpha$  exposure in 3 of the 4 MPN patients who carried both *JAK2-V617F*

and *DNMT3A* mutations, whereas the percentages of *JAK2-V617F* positive colonies decreased or remained unchanged in patients carrying solely *JAK2-V617F* (Figure 5C and D). Overall, the responses of the primary human HSPCs from MPN patients to IFN $\alpha$  are in line with the results obtained in our MPN mouse models.

### **Treatment with pegIFN $\alpha$ induces stronger response in *VF;Dm $\Delta/\Delta$* LT-HSCs in vivo**

To analyze if *VF* and *VF;Dm $\Delta/\Delta$*  LT-HSCs respond differentially to IFN $\alpha$ , we injected *VF* and *VF;Dm $\Delta/\Delta$*  mice with a single dose of non-pegylated IFN $\alpha$  (25  $\mu$ g/kg) or vehicle, and sorted phenotypic LT-HSCs after 24 hours for single-cell RNAseq (Figure 6A). Unsupervised clustering of sorted cells identified 9 clusters, which were grouped into 6 different cell populations based on lineage-specific gene expression patterns (Figure 6B-C and Supplemental Figure S11).<sup>34</sup> We observed a shift towards more differentiated clusters upon treatment with IFN $\alpha$  in both genotypes (Figure 6D). We then focused on expression changes in the most naive cluster of quiescent LT-HSCs (Figure 6E-H). Expression of genes involved in IFN-response was significantly elevated in quiescent LT-HSCs from *VF;Dm $\Delta/\Delta$*  mice compared to *VF* mice (Figure 6E and F). Furthermore, analysis of chemokines (*Cxcl9* and *Cxcl10*), previously shown to be directly induced by IFN-signaling,<sup>35-37</sup> showed significantly higher expression only in *VF;Dm $\Delta/\Delta$*  quiescent LT-HSCs (Figure 6G). In line with these results, the analysis of activities of several signaling pathways in each single cell using the tool PROGENy showed increased Jak-Stat, NF $\kappa$ B and TNF $\alpha$  signaling in quiescent LT-HSCs from *VF;Dm $\Delta/\Delta$*  mice compared to *VF* mice treated with IFN $\alpha$  (Figure 6H), indicating more robust response to IFN in double mutant quiescent LT-HSCs.

### ***VF;Dm $\Delta/\Delta$* mice showed improved response to a combination of pegIFN $\alpha$ with 5-azacytidine**

We examined whether the resistance of double mutant *VF;Dm $\Delta/\Delta$*  mice to pegIFN $\alpha$  can be overcome by addition of either arsenic trioxide (At), which was shown to potentiate IFN $\alpha$ -induced growth suppression of *JAK2-V617F* hematopoietic progenitors,<sup>38</sup> or 5-azacytidine (Aza) that interferes with DNA methylation of cytidine,<sup>39</sup> and showed increased cytotoxicity in the presence of *Dnmt3a* mutations.<sup>40,41</sup> To test the effects of the

treatments *in vivo*, we generated cohorts of mice using competitive transplantations of BM cells from *VF* or *VF;Dm<sup>Δ/Δ</sup>* mice that express a GFP reporter gene mixed with a 10-fold excess of BM cells from a *WT* mouse and into lethally irradiated *WT* recipient mice (Figure 7A). After 7 weeks, recipient mice were randomized into 6 treatment groups and were treated for 12 weeks either with pegIFN $\alpha$  (25 $\mu$ g/kg; s.c. once per week), At (5mg/kg; i.p. every second day), or Aza (2mg/kg; i.p. daily) for two weeks followed by a break of 2 weeks (Figure 7A). In addition, we tested the combinations of pegIFN $\alpha$ +At and pegIFN $\alpha$ +Az. No significant changes in body weight were observed compared with the vehicle treated group, except in mice treated with pegIFN $\alpha$ +At (Figure 7B). Spleen and liver weight was decreased in all treatment groups and genotypes (Figure 7C and D), except in *VF;Dnmt3a<sup>Δ/Δ</sup>* mice treated with pegIFN $\alpha$  alone, which showed a trend towards increased spleen and liver weights. Blood counts were normalized in all treatment groups (Figure 7E). The combinations of pegIFN $\alpha$ +At and pegIFN $\alpha$ +Aza also induced pronounced decrease in GFP-chimerism in peripheral blood lineages of *VF* mice, while *VF;Dnmt3a<sup>Δ/Δ</sup>* mice were largely resistant and only the combination of pegIFN $\alpha$ +Aza was effective in reducing the GFP-chimerism (Figure 7E). The frequencies of LT-HSC and their GFP-chimerism in BM and spleen are shown in Figure 7F. In *VF* mice, treatment arms that contained pegIFN $\alpha$  increased the overall frequencies of LT-HSCs primarily by increasing the proportion of GFP-negative (*JAK2*-wildtype) cells. The strongest reduction in GFP-chimerism was observed in *VF* mice treated with a combination of pegIFN $\alpha$ +Aza (Figure 7F). LT-HSC from *VF;Dm<sup>Δ/Δ</sup>* mice were largely resistant and showed reduction in GFP-chimerism only when treated with a combination of pegIFN $\alpha$ +Aza (Figure 7F).

To test the effects of the different treatments on the capacity of LT-HSCs to remain functional and maintain MPN, we performed non-competitive transplantations into secondary recipients using BM cells harvested and pooled from 3 mice per group at the end of the treatments (Supplemental Figure S12A). BM from *VF* mice treated with vehicle caused PV phenotype in secondary recipients with splenomegaly and high GFP-chimerism in peripheral blood cells (Supplemental Figure S12B and C). All treatments reduced the capacity of *VF* BM cells to induce MPN phenotype in secondary recipients

and the combination of pegIFN $\alpha$ +Aza was most effective in reducing GFP-chimerism in peripheral blood and LT-HSCs in BM and spleen (Supplemental Figure S12D). In contrast, none of the treatments impaired the capacity of BM cells from double mutant *VF;Dm $\Delta/\Delta$*  mice to induce MPN phenotype in secondary recipients and despite a temporary decrease in GFP-chimerism, at 16 weeks the *JAK2*-mutant cells dominated in peripheral blood, and only a small decrease in chimerism was noted in LT-HSCs in BM and spleen of mice transplanted with cells from pegIFN $\alpha$  or Aza treated mice (Supplemental Figure S12D).

To further characterize the effects of pegIFN $\alpha$ , Aza and pegIFN $\alpha$ +Aza of LT-HSCs, we performed an additional transplantation experiment and analyzed the changes in cell cycle, DNA damage, and the transcriptome (Supplemental Figures S13 and S14). The cell cycle and DNA damage analyses were performed separately on GFP-positive (*JAK2*-mutant) and GFP-negative (*WT*) LT-HSCs. In *VF* and in *VF;Dm $\Delta/\Delta$*  mice, IFN $\alpha$ +Aza strongly reduced *JAK2*-mutant and *WT* LT-HSCs in G0 and increased HSCs in G1 and S/G2/M phase, while the single agents had either a weak or no significant effect on cell cycle (Supplemental Figure S13D). Similar increase in DNA damage was observed in GFP-positive (*JAK2*-mutant) LT-HSCs, but not in GFP-negative (*WT*) HSCs (Supplemental Figure S13E), suggesting that *WT* HSCs can cope better with the proliferation-induced stress caused by IFN $\alpha$ . Our RNAseq data in sorted LT-HSCs (Supplemental Figure S14) revealed that in single mutant *VF* HSCs, IFN $\alpha$  and Aza as single agents upregulated only the IFN- / inflammatory responses, or the *E2F* and *Myc* pathways, respectively, whereas the combo of IFN $\alpha$ +Aza had additive effects, upregulating both IFN- / inflammatory responses as well as *E2F* and *Myc* pathways, without increasing the relative -fold changes. In contrast, in the double mutant *VF;Dm $\Delta/\Delta$*  HSCs, we observed upregulation of *E2F* and *Myc* pathways already in HSCs treated with IFN $\alpha$  alone, and upregulation of the IFN-responses already in HSCs treated with Aza alone. In the HSCs treated with the combo, we saw IFN-responses and *E2F/Myc* pathways to be both upregulated to higher fold-levels than in HSCs treated with the single agents.



Overall, the combination of pegIFN $\alpha$ +Aza partially overcame resistance to pegIFN $\alpha$  alone in primary *VF;Dm $\Delta/\Delta$*  mice (Figure 7), but BM from these treated mice recovered and induced high platelet counts in secondary recipients. Interestingly, pegIFN $\alpha$ +Aza strongly decreased the *JAK2*-mutant allele burden single mutant *VF* mice, and prevented initiation of MPN in secondary recipients, showing potential to inflict long-term damage preferentially to the *JAK2*-mutant clone.

## Discussion

Non-transplanted *VF;Dm<sup>ΔΔ</sup>* mice displayed milder MPN phenotype with less pronounced splenomegaly, lower blood counts and lower grade of myelofibrosis compared with non-transplanted *VF* mice (Figure 1). The phenotype in recipients of BM from *VF;Dm<sup>ΔΔ</sup>* mice was comparable to non-transplanted *VF;Dm<sup>ΔΔ</sup>* mice, but was more pronounced with higher platelet counts and higher degree of myelofibrosis than in recipients of BM from *VF* mice (Figure 2 and Supplemental Figure S6). The accentuated phenotype in recipients transplanted with *VF;Dm<sup>ΔΔ</sup>* BM appears to be related to the expansion of LT-HSCs and early progenitors under stress the recovery after transplantation (Figure 2E).<sup>16</sup> The competitive advantage and increased self-renewal potential of the double mutant *VF;Dm<sup>ΔΔ</sup>* HSCs was further evident in secondary and tertiary transplantations, resulting in more aggressive disease (Figure 4).

The phenotype of our *VF;Dm<sup>ΔΔ</sup>* mice showed similarities but also some differences with the phenotypes of previously described *E2ACre;Jak2<sup>V617F</sup>* knockin (*E2Ki*) mice, in which mutations in the *Dnmt3a* methyltransferase domain were induced by CRISPR-Cas9 gene-editing.<sup>42</sup> The unmodified *E2Ki* mice had high hematocrit, but normal platelet and neutrophil counts,<sup>42,43</sup> whereas our *VF* mice display elevated hematocrit with high platelet and neutrophil counts.<sup>23,44</sup> The effects of CRISPR-Cas9 induced loss of *Dnmt3a* in *E2Ki* mice was studied using BM transplantations and should therefore be compared with our transplantations of *VF;Dm<sup>ΔΔ</sup>* BM. The *Dnmt3a* protein was not detected in *Dnmt3a-Cas9* targeted BM cells (Suppl. Figure S1B in Ref.<sup>42</sup>), consistent with biallelic loss of *Dnmt3a*. *VF;Dm<sup>ΔΔ</sup>* and *E2Ki;Dnmt3a-Cas9* mice both displayed higher degree of myelofibrosis compared to mutant *VF* or *E2Ki* mice. However, *E2Ki;Dnmt3a-Cas9* mice displayed higher spleen weight but decreased frequencies of LT-HSCs,<sup>42</sup> compared to our *VF;Dm<sup>ΔΔ</sup>* mice. The expansion of phenotypic and functional LT-HSCs in our *VF;Dm<sup>ΔΔ</sup>* mice is in line with the well documented expansion of HSCs in *Dnmt3a* knockout mice.<sup>15-</sup>

17

PegIFN $\alpha$  largely normalized blood counts in recipients of *VF* and *VF;Dm<sup>ΔΔ</sup>* BM cells, but was unable to substantially reduce the *JAK2*-mutant allele burden in HSPC of

*VF;Dm<sup>ΔΔ</sup>* mice (Figure 2E-F and Supplemental Figure S4). Primary recipients of *VF;Dm<sup>ΔΔ</sup>* BM already showed signs of adverse outcome in the pegIFN $\alpha$  arm, e.g. a trend towards increased spleen weight compared to vehicle (Figure 2D). The aggravating impact of IFN $\alpha$  on *VF;Dm<sup>ΔΔ</sup>* hematopoiesis was even more apparent in secondary transplantations, with increased platelet counts, increased chimerism in peripheral blood lineages and vastly expanded HSPC pool composed exclusively of mutant cells (Figure 4). Consistent with the mouse data, we also observed adverse effects to IFN $\alpha$  in primary hematopoietic progenitors from patients with *JAK2-V617F* and *DNMT3A* mutations (Figure 5). MPN patients with *JAK2-V617F* and *DNMT3A* mutations were reported to respond less to IFN $\alpha$  treatment,<sup>45</sup> and to show expansion of subclones with *JAK2-V617F* and *DNMT3A* mutations under IFN $\alpha$  treatment.<sup>46</sup>

Previous studies in mice have shown that long-term treatment with pegIFN $\alpha$  preferentially targets *Jak2-V617F* LT-HSCs.<sup>20,21</sup> Direct effects of IFN $\alpha$  on wildtype LT-HSCs were linked to cell cycle activation and replication-induced stress, resulting in LT-HSC exhaustion,<sup>31</sup> in line with the previous reports of replication stress being a critical factor in the functional decline of LT-HSC.<sup>47</sup> More recently, long-term pegIFN $\alpha$  treatment was shown to preferentially affect *Jak2-V617F* LT-HSCs over *WT* LT-HSCs through sustained loss of quiescence, ROS production and DNA damage accumulation.<sup>22</sup>

Our data show that LT-HSCs and early hematopoietic progenitors from double-mutant *VF;Dm<sup>ΔΔ</sup>* mice treated with IFN $\alpha$  were largely resistant to the accumulation of DNA damage, ROS, and exit of dormancy compared to *VF* (Figure 3). In secondary transplantations, LT-HSCs from IFN $\alpha$  treated *VF;Dm<sup>ΔΔ</sup>* mice showed increased self-renewal potential, resulting paradoxically in more aggressive disease (Figure 4). RNAseq data from sorted LT-HSCs, showed upregulation of inflammatory signatures in pegIFN $\alpha$  treated *VF* and *VF;Dm<sup>ΔΔ</sup>* mice (Figure 6 and Supplemental Figure S14). Thus, *VF;Dm<sup>ΔΔ</sup>* HSCs were capable of maintaining their stemness despite exhibiting a greater upregulation of inflammatory pathways upon IFN $\alpha$  treatment, compared to single mutant *VF* HSCs. This suggests that the loss of *Dnmt3a* increases the threshold at which the double mutant HSCs begin to exhaust when exposed to IFN $\alpha$  signaling. Inflammation

mediated by IFN-gamma or TNF $\alpha$  was also reported to promote the expansion of *DNMT3A* mutant clones in *JAK2*-wildtype hematopoiesis.<sup>48,49</sup> Thus, resistance was not due to a block in IFN action, to the contrary, signaling was strongly activated by IFN $\alpha$ , but loss of Dnmt3a protected the double mutant HSCs from the deleterious effects of increased IFN signaling.

Combinations of pegIFN $\alpha$ +At and pegIFN $\alpha$ +Aza were very effective and pegIFN $\alpha$ +Aza almost completely eliminated the *JAK2*-mutant clone in mice carrying the *VF* mutation alone (Figure 7 and Supplemental Figures S12 and S13). RNAseq data in sorted LT-HSCs (Supplemental Figure S14) showed that IFN $\alpha$ +Aza had the strongest effect on upregulating IFN- and inflammatory responses, as well as E2F and Myc pathways, which promote cell division and differentiation,<sup>50</sup> ultimately contributing to exhausting the *VF* clone. Compared to *VF* mice, *VF;Dm $\Delta/\Delta$*  mice treated with pegIFN $\alpha$ +Aza showed enhanced upregulation of IFN-responses and E2F/Myc pathways in LT-HSCs, but responded with only ~50% reduction of *JAK2*-617F-chimerism, and fully recovered MPN phenotype in secondary transplantations.

Overall, our data show that MPN caused by *JAK2*-V617F combined with loss of *Dnmt3a* resulted in a robust MPN phenotype, which worsened when the *VF;Dm $\Delta/\Delta$*  mutant HSCs were exposed to external stress, such as transplantation or treatment with pegIFN $\alpha$ . Therefore, pegIFN $\alpha$  should be avoided or applied with caution in patients who carry *JAK2*-V617F and *DNMT3A* mutations in the same clone. The combination of pegIFN $\alpha$ +Aza partially overcame resistance in *VF;Dm $\Delta/\Delta$*  mice and strongly decreased the *JAK2*-mutant allele burden in mice carrying *VF* mutation only, rendering the HSCs incapable of initiating MPN in secondary recipients. The combination of pegIFN $\alpha$ +Aza therefore bears promise for the treatment of patients with MPN caused by *JAK2*-V617F without presence of additional somatic gene mutations.

## **AUTHOR CONTRIBUTIONS**

MU and JS designed and performed research, analyzed data and wrote the manuscript, DLP, NH, QK, TAF, ML, LK, RK and HHS, performed research and analyzed data, AB, AT, JS, JCL and SD analyzed data, RCS designed research, analyzed data and wrote the manuscript.

## **ACKNOWLEDGMENTS**

We thank Dr. David Tough for providing the NS0 cell line engineered to overproduce mouse IFN $\alpha$ 4 and Albert Neutzner for help with the FPLC purification of IFN $\alpha$ . We also thank the Genomics Facility of the University of Basel for the help with RNA preparation for single-cell and bulk RNAseq and members of the laboratory for helpful discussions and critical reading of our manuscript.

## **GRANT SUPPORT**

This work was supported by grants from the Swiss National Science Foundation (31003A\_166613, 310030\_185297/1, and 310030\_185297/2) and Swiss Cancer Research (KFS-3655-02-2015 and KFS-4462-02-2018), and the Stiftung für Hämatologische Forschung to RCS, and by the Czech Science Foundation grant 17-05988S to J.S.

## **DECLARATION OF INTERESTS**

R.C.S. is a scientific advisor/SAB member and has equity in Ajax Therapeutics, he consulted for and/or received honoraria from Novartis, BMS/Celgene, AOP, GSK, Baxalta and Pfizer. N.H. owns stocks in the company Cantargia. The remaining authors declare no competing financial interests.

## References

1. Vainchenker W, Kralovics R. Genetic basis and molecular pathophysiology of classical myeloproliferative neoplasms. *Blood*. 2017;129(6):667-679.
2. Lundberg P, Karow A, Nienhold R, et al. Clonal evolution and clinical correlates of somatic mutations in myeloproliferative neoplasms. *Blood*. 2014;123(14):2220-2228.
3. Guglielmelli P, Lasho TL, Rotunno G, et al. The number of prognostically detrimental mutations and prognosis in primary myelofibrosis: an international study of 797 patients. *Leukemia*. 2014;28(9):1804-1810.
4. Guglielmelli P, Lasho TL, Rotunno G, et al. MIPSS70: Mutation-Enhanced International Prognostic Score System for Transplantation-Age Patients With Primary Myelofibrosis. *J Clin Oncol*. 2018;36(4):310-318.
5. Grinfeld J, Nangalia J, Baxter EJ, et al. Classification and Personalized Prognosis in Myeloproliferative Neoplasms. *N Engl J Med*. 2018;379(15):1416-1430.
6. Luque Paz D, Jouanneau-Courville R, Riou J, et al. Leukemic evolution of polycythemia vera and essential thrombocythemia: genomic profiles predict time to transformation. *Blood Adv*. 2020;4(19):4887-4897.
7. Jaiswal S, Fontanillas P, Flannick J, et al. Age-related clonal hematopoiesis associated with adverse outcomes. *N Engl J Med*. 2014;371(26):2488-2498.
8. Genovese G, Kahler AK, Handsaker RE, et al. Clonal hematopoiesis and blood-cancer risk inferred from blood DNA sequence. *N Engl J Med*. 2014;371(26):2477-2487.
9. Xie M, Lu C, Wang J, et al. Age-related mutations associated with clonal hematopoietic expansion and malignancies. *Nat Med*. 2014;20(12):1472-1478.
10. Shlush LI, Zandi S, Mitchell A, et al. Identification of pre-leukaemic haematopoietic stem cells in acute leukaemia. *Nature*. 2014;506(7488):328-333.
11. Corces-Zimmerman MR, Hong WJ, Weissman IL, Medeiros BC, Majeti R. Preleukemic mutations in human acute myeloid leukemia affect epigenetic regulators and persist in remission. *Proc Natl Acad Sci U S A*. 2014;111(7):2548-2553.
12. Yang L, Rau R, Goodell MA. DNMT3A in haematological malignancies. *Nat Rev Cancer*. 2015;15(3):152-165.
13. Russler-Germain DA, Spencer DH, Young MA, et al. The R882H DNMT3A mutation associated with AML dominantly inhibits wild-type DNMT3A by blocking its ability to form active tetramers. *Cancer Cell*. 2014;25(4):442-454.
14. Spencer DH, Russler-Germain DA, Ketkar S, et al. CpG Island Hypermethylation Mediated by DNMT3A Is a Consequence of AML Progression. *Cell*. 2017;168(5):801-816 e813.
15. Challen GA, Sun D, Jeong M, et al. Dnmt3a is essential for hematopoietic stem cell differentiation. *Nat Genet*. 2011;44(1):23-31.
16. Jeong M, Park HJ, Celik H, et al. Loss of Dnmt3a Immortalizes Hematopoietic Stem Cells In Vivo. *Cell Rep*. 2018;23(1):1-10.
17. Ostrander EL, Kramer AC, Mallaney C, et al. Divergent Effects of Dnmt3a and Tet2 Mutations on Hematopoietic Progenitor Cell Fitness. *Stem Cell Reports*. 2020;14(4):551-560.
18. Kiladjian JJ, Cassinat B, Chevret S, et al. Pegylated interferon-alfa-2a induces complete hematologic and molecular responses with low toxicity in polycythemia vera. *Blood*. 2008;112(8):3065-3072.

19. Quintas-Cardama A, Kantarjian H, Manshouri T, et al. Pegylated interferon alfa-2a yields high rates of hematologic and molecular response in patients with advanced essential thrombocythemia and polycythemia vera. *J Clin Oncol*. 2009;27(32):5418-5424.
20. Mullally A, Bruedigam C, Poveromo L, et al. Depletion of Jak2V617F myeloproliferative neoplasm-propagating stem cells by interferon-alpha in a murine model of polycythemia vera. *Blood*. 2013;121(18):3692-3702.
21. Hasan S, Lacout C, Marty C, et al. JAK2V617F expression in mice amplifies early hematopoietic cells and gives them a competitive advantage that is hampered by IFNalpha. *Blood*. 2013;122(8):1464-1477.
22. Austin RJ, Straube J, Bruedigam C, et al. Distinct effects of ruxolitinib and interferon-alpha on murine JAK2V617F myeloproliferative neoplasm hematopoietic stem cell populations. *Leukemia*. 2020;34(4):1075-1089.
23. Tiedt R, Hao-Shen H, Sobas MA, et al. Ratio of mutant JAK2-V617F to wild-type Jak2 determines the MPD phenotypes in transgenic mice. *Blood*. 2008;111(8):3931-3940.
24. Kaneda M, Okano M, Hata K, et al. Essential role for de novo DNA methyltransferase Dnmt3a in paternal and maternal imprinting. *Nature*. 2004;429(6994):900-903.
25. Schaefer BC, Schaefer ML, Kappler JW, Marrack P, Kiedl RM. Observation of antigen-dependent CD8+ T-cell/ dendritic cell interactions in vivo. *Cell Immunol*. 2001;214(2):110-122.
26. Gothert JR, Gustin SE, Hall MA, et al. In vivo fate-tracing studies using the Scl stem cell enhancer: embryonic hematopoietic stem cells significantly contribute to adult hematopoiesis. *Blood*. 2005;105(7):2724-2732.
27. Le Bon A, Etchart N, Rossmann C, et al. Cross-priming of CD8+ T cells stimulated by virus-induced type I interferon. *Nat Immunol*. 2003;4(10):1009-1015.
28. Khoury JD, Solary E, Abla O, et al. The 5th edition of the World Health Organization Classification of Haematolymphoid Tumours: Myeloid and Histiocytic/Dendritic Neoplasms. *Leukemia*. 2022;36(7):1703-1719.
29. Rao TN, Hansen N, Stetka J, et al. JAK2-V617F and interferon-alpha induce megakaryocyte-biased stem cells characterized by decreased long-term functionality. *Blood*. 2021;137(16):2139-2151.
30. Burma S, Chen BP, Murphy M, Kurimasa A, Chen DJ. ATM phosphorylates histone H2AX in response to DNA double-strand breaks. *J Biol Chem*. 2001;276(45):42462-42467.
31. Walter D, Lier A, Geiselhart A, et al. Exit from dormancy provokes DNA-damage-induced attrition in haematopoietic stem cells. *Nature*. 2015;520(7548):549-552.
32. Tasdogan A, Kumar S, Allies G, et al. DNA Damage-Induced HSPC Malfunction Depends on ROS Accumulation Downstream of IFN-1 Signaling and Bid Mobilization. *Cell Stem Cell*. 2016;19(6):752-767.
33. Hu Y, Smyth GK. ELDA: extreme limiting dilution analysis for comparing depleted and enriched populations in stem cell and other assays. *J Immunol Methods*. 2009;347(1-2):70-78.
34. Rodriguez-Fraticelli AE, Wolock SL, Weinreb CS, et al. Clonal analysis of lineage fate in native haematopoiesis. *Nature*. 2018;553(7687):212-216.

35. Luster AD, Unkeless JC, Ravetch JV. Gamma-interferon transcriptionally regulates an early-response gene containing homology to platelet proteins. *Nature*. 1985;315(6021):672-676.
36. Cole KE, Strick CA, Paradis TJ, et al. Interferon-inducible T cell alpha chemoattractant (I-TAC): a novel non-ELR CXC chemokine with potent activity on activated T cells through selective high affinity binding to CXCR3. *J Exp Med*. 1998;187(12):2009-2021.
37. Padovan E, Spagnoli GC, Ferrantini M, Heberer M. IFN-alpha2a induces IP-10/CXCL10 and MIG/CXCL9 production in monocyte-derived dendritic cells and enhances their capacity to attract and stimulate CD8+ effector T cells. *J Leukoc Biol*. 2002;71(4):669-676.
38. Dagher T, Maslah N, Edmond V, et al. JAK2V617F myeloproliferative neoplasm eradication by a novel interferon/arsenic therapy involves PML. *J Exp Med*. 2021;218(2).
39. Im AP, Sehgal AR, Carroll MP, et al. DNMT3A and IDH mutations in acute myeloid leukemia and other myeloid malignancies: associations with prognosis and potential treatment strategies. *Leukemia*. 2014;28(9):1774-1783.
40. Chiappinelli KB, Strissel PL, Desrichard A, et al. Inhibiting DNA Methylation Causes an Interferon Response in Cancer via dsRNA Including Endogenous Retroviruses. *Cell*. 2015;162(5):974-986.
41. Scheller M, Ludwig AK, Gollner S, et al. Hotspot DNMT3A mutations in clonal hematopoiesis and acute myeloid leukemia sensitize cells to azacytidine via viral mimicry response. *Nat Cancer*. 2021;2(5):527-544.
42. Jacquelin S, Straube J, Cooper L, et al. Jak2V617F and Dnmt3a loss cooperate to induce myelofibrosis through activated enhancer-driven inflammation. *Blood*. 2018;132(26):2707-2721.
43. Mullally A, Lane SW, Ball B, et al. Physiological Jak2V617F expression causes a lethal myeloproliferative neoplasm with differential effects on hematopoietic stem and progenitor cells. *Cancer Cell*. 2010;17(6):584-596.
44. Kubovcakova L, Lundberg P, Grisouard J, et al. Differential effects of hydroxyurea and INC424 on mutant allele burden and myeloproliferative phenotype in a JAK2-V617F polycythemia vera mouse model. *Blood*. 2013;121(7):1188-1199.
45. Quintas-Cardama A, Abdel-Wahab O, Manshour T, et al. Molecular analysis of patients with polycythemia vera or essential thrombocythemia receiving pegylated interferon alpha-2a. *Blood*. 2013;122(6):893-901.
46. Knudsen TA, Skov V, Stevenson K, et al. Genomic profiling of a randomized trial of interferon-alpha vs hydroxyurea in MPN reveals mutation-specific responses. *Blood Adv*. 2022;6(7):2107-2119.
47. Flach J, Bakker ST, Mohrin M, et al. Replication stress is a potent driver of functional decline in ageing haematopoietic stem cells. *Nature*. 2014;512(7513):198-202.
48. Hormaechea-Agulla D, Matatall KA, Le DT, et al. Chronic infection drives Dnmt3a-loss-of-function clonal hematopoiesis via IFNgamma signaling. *Cell Stem Cell*. 2021;28(8):1428-1442 e1426.
49. SanMiguel JM, Eudy E, Loberg MA, et al. Distinct Tumor Necrosis Factor Alpha Receptors Dictate Stem Cell Fitness versus Lineage Output in Dnmt3a-Mutant Clonal Hematopoiesis. *Cancer Discov*. 2022;12(12):2763-2773.



50. Wilson A, Murphy MJ, Oskarsson T, et al. c-Myc controls the balance between hematopoietic stem cell self-renewal and differentiation. *Genes Dev.* 2004;18(22):2747-2763.

## Figure legends

### Figure 1. Disease phenotype characterization of *JAK2-V617F* (*VF*) and *JAK2-V617F;Dnmt3a<sup>Δ/Δ</sup>* (*VF;Dm<sup>Δ/Δ</sup>*) mice.

(A) Schematic drawing of induction with tamoxifen injections for 4 weeks (orange box) and experimental procedures. CBC, complete blood count; *WT*, *wildtype*; *VF*, *JAK2-V617F*; *Dm<sup>Δ/Δ</sup>*, *Dnmt3a<sup>Δ/Δ</sup>* (B) Analysis of Cre-mediated excision of *Dnmt3a*. Left panel shows representative gel from Bioanalyzer DNA chip, with bands corresponding to floxed (*fl*) and deleted ( $\Delta$ ) *Dnmt3a* alleles. Right panel shows quantification of *fl* and  $\Delta$  *Dnmt3a* alleles (n=4 per genotype). (C) Time course of non-fasting blood glucose levels (n=5-7 mice per genotype). (D) Time course of peripheral blood counts (n=5-7 mice per genotype). (E) Spleen weight at terminal workup after 16 weeks post-induction. (F) Bone marrow (BM) cellularity per 4 bones (n=4-5 mice per genotype). (G) Frequencies of hematopoietic stem and progenitor cells (HSPCs) in bone marrow and spleen at terminal workup after 16 weeks of treatment (n=4-5 mice per genotype). (H) Analysis of erythroid progenitor's frequencies in bone marrow and spleen at terminal analysis. (I) Quantification bone marrow fibrosis and osteosclerosis (n=4-5 mice per genotype). The degree of myelofibrosis was scored and assigned on a scale from MF-0 to MF-3. Osteosclerosis was scored as present or absent. All data are presented as mean  $\pm$  standard error of the mean. Two-way analyses of variance (ANOVAs) with subsequent Tukey (B, C) and Dunnett posttest (G – Erythroid progenitors), One-way ANOVAs with subsequent Tukey posttest (D, E, G – Ter119<sup>+</sup> cells, H) or Unpaired *t* test with Welch's correction (F) were used. \*P < .05, \*\*P < .01, \*\*\*P < .001, \*\*\*\*P < .0001.

### Figure 2. Differential effects of pegylated IFN $\alpha$ on hematopoiesis in *JAK2-V617F* (*VF*) and *JAK2-V617F;Dnmt3a<sup>Δ/Δ</sup>* (*VF;Dm<sup>Δ/Δ</sup>*) mice.

(A) Schematic drawing of the experimental setup for bone marrow (BM) transplantations and treatment with pegIFN $\alpha$ . (B) Time course of body weight (n=24 mice per group). (C) Time course of blood counts and GFP-chimerism of recipient mice (n = 24 mice per group). (D) Spleen weight at terminal workup after 16 weeks of treatment. (E) Frequency and GFP-chimerism of *VF;GFP* or *VF;Dm<sup>Δ/Δ</sup>;GFP* hematopoietic stem and progenitor

cells (HSPCs) in bone marrow at terminal workup after 16 weeks of treatment (n = 15 mice per group). (F) Frequency and GFP-chimerism of *VF;GFP* or *VF;Dm<sup>Δ/Δ</sup>;GFP* hematopoietic stem and progenitor cells (HSPCs) in spleen at terminal workup after 16 weeks of treatment (n = 15 mice per group). (G) Analysis of the proportions of CD41<sup>hi</sup> and CD41<sup>lo</sup> subpopulations within the mutant (GFP-positive) LT-HSCs. All data are presented as mean ± standard error of the mean. Two-way analyses of variance (ANOVAs) with subsequent Tukey (C, E, F, G) posttest or One-way ANOVAs with subsequent Tukey (D) posttest were used. \*P < .05, \*\*P < .01, \*\*\*P < .001, \*\*\*\*P < .0001.

**Figure 3. Effects of IFN $\alpha$  treatment on accumulation of DNA damage and reactive oxygen species, and on cell division in hematopoietic stem and progenitor cells.**

(A) Accumulation of reactive oxygen species (ROS) and presence of  $\gamma$ H2AX in *lin<sup>-</sup>/Sca1<sup>+</sup>/Kit<sup>+</sup>* (LSK) cells from bone marrow (BM) and spleen of recipient mice. GFP-chimerism in LSK cells, gating strategy and detection of DNA damage by anti- $\gamma$ H2AX antibody and ROS by staining with CellRox is shown on the left. Quantification of  $\gamma$ H2AX and ROS in 9 mice per group is shown in the right panel. (B) Analysis of cell division (Ki67-positive cells) and DNA damage within the mutant (GFP-positive) LT-HSCs. Left panel shows the LT-HSC chimerism and gating strategy. Right panel shows the results obtained from 9 mice per group. (C) Analysis of ROS levels in GFP-positive LT-HSCs. This data was obtained from mice described in Supplemental Figure S13. All data are presented as mean ± standard error of the mean. Two-way analysis of variance (ANOVAs) with subsequent Tukey posttest was used. \*\*P < .01, \*\*\*P < .001, \*\*\*\*P < .0001.

**Figure 4. Transplantations of bone marrow cells from primary recipients into secondary recipients.**

(A) Schematic drawing of the experimental setup for non-competitive bone marrow (BM) transplantations into secondary recipient mice (n=6 mice per group). (B) Percentages of mice that showed engraftment defined as >1% GFP-chimerism in Gr1<sup>+</sup> cells in peripheral blood at 20 weeks post transplantation. (C) Spleen weight at terminal workup

20 weeks post transplantation. **(D)** Time course of blood counts and GFP-chimerism in secondary recipients. **(E)** GFP-chimerism in LT-HSCs at terminal workup 20 weeks post transplantation. **(F)** Schematic drawing of the experimental setup for competitive bone marrow transplantations into secondary recipients at 1:50 dilution (n=12 mice per group). **(G-J)** Same annotations as in B-E. Two-way analyses of variance (ANOVAs) with subsequent Tukey (D, I) posttest or One-way ANOVAs with subsequent Tukey (E, H) posttest were used. \*P < .05, \*\*P < .01, \*\*\*P < .001, \*\*\*\*P < .0001.

**Figure 5. Effects of IFN $\alpha$  on hematopoietic stem and progenitor cells (HSPCs) from MPN patients carrying *JAK2-V617F* and *DNMT3A* mutations.**

**(A)** Experimental setup for liquid cultures of single cell FACS sorted hematopoietic stem and progenitor cells (HSPCs). **(B)** Growth efficiency of single cell sorted HSPCs expressed as the percentages of wells in which colonies grew. **(C)** Genotyping of HSPC-derived colonies treated with IFN $\alpha$  or vehicle. Stacked bars represent the percentages of colonies for each of the genotypes. Numbers above the bars indicate the numbers of colonies analyzed. **(D)** Relative change (%) in the numbers of *JAK2-V617F*<sup>+</sup> colonies. Two-way analyses of variance (ANOVAs) with subsequent Sidak (D) posttest were used.

**Figure 6. Differential effects of IFN $\alpha$  treatment on *VF* and *VF;Dm<sup>4/4</sup>* LT-HSCs**

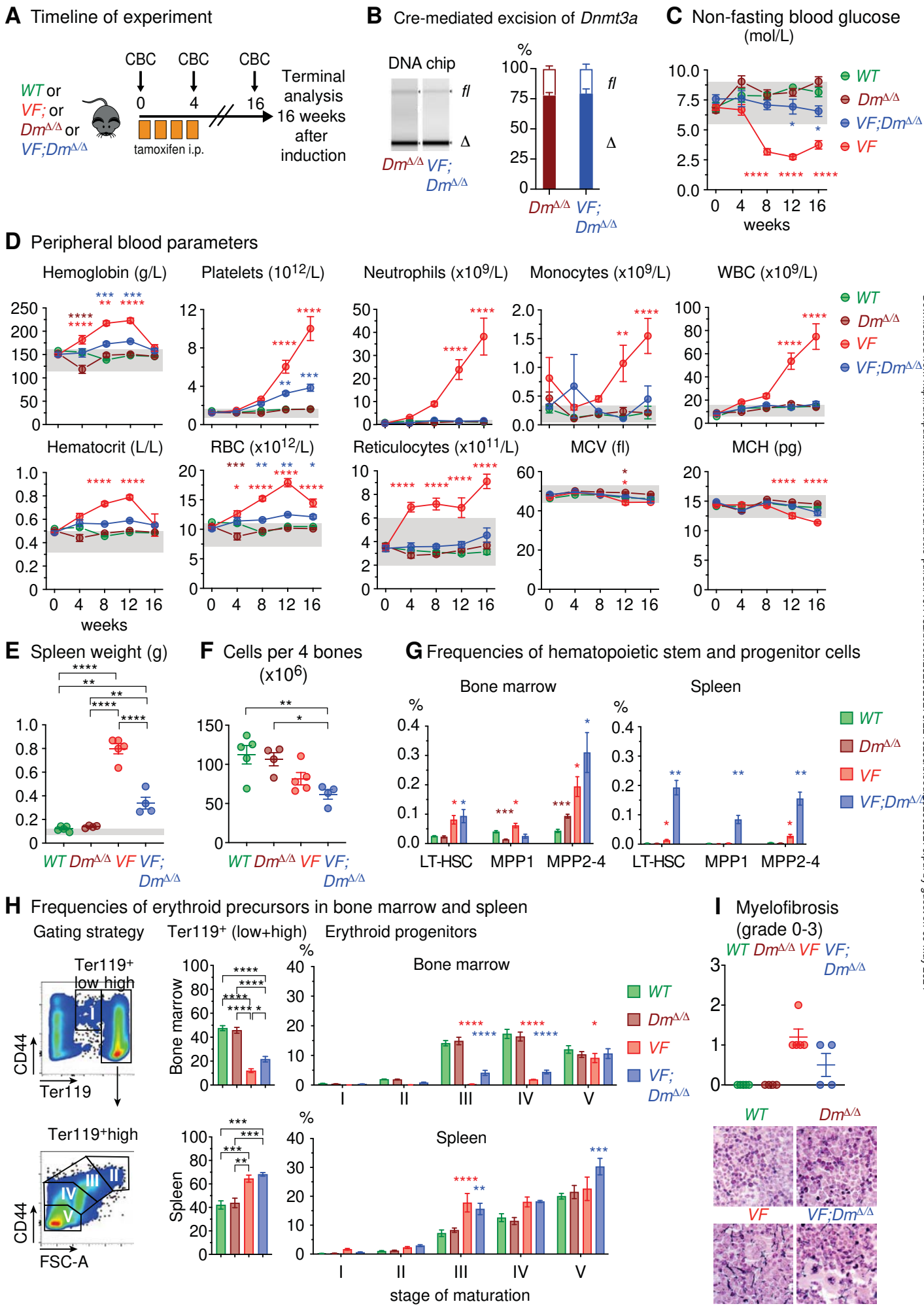
**(A)** Experimental setup for single-cell RNA seq of FACS sorted long-term hematopoietic stem cells (LT-HSCs). **(B)** Expression of selected lineage and cycling genes in reduced dimension plots. TSNE, t-distributed stochastic neighbor embedding. **(C)** Clustering of cells is based on the gene expression in reduced dimension plot **(D)** Left panel depicts shifts in cell identity induced by IFN $\alpha$  treatment in reduced dimension plots. Right panel shows the relative cell abundance per cell type across genotypes and treatments. **(E)** Heatmap analysis of IFN response genes expression (Reactome R-MMU-91353) in quiescent LT-HSCs. Normalized expression of genes in pseudo-bulk samples was plotted. **(F)** Gene set enrichment analysis (GSEA) of Hallmark gene sets comparing IFN $\alpha$ -treated *VF* and *VF;Dm<sup>4/4</sup>* quiescent LT-HSCs (qLT-HSCs). **(G)** Fold change in the normalized expression of *Cxcl9* and *Cxcl10* genes derived from number of reads (CPM) in pseudo-bulk analysis. Expression in vehicle treated *VF* cells was set to 1. **(H)** Pathway

RespOnsive GENes for activity inference analysis (Progeny) in quiescent LT-HSCs. Two-way analysis of variance (ANOVAs) with subsequent Tukey posttest was used. \*\*P < .01, \*\*\*P < .001, \*\*\*\*P < .0001.

**Figure 7. Treatment with combination of 5-azacytidine or arsenic trioxide with pegIFN $\alpha$**

(A) Schematic drawing of the experimental setup for bone marrow (BM) transplantations and treatment. (B) Time course of changes in body weight (%). N = 6-8 per group. (C) Spleen weight at terminal workup after 12 weeks of treatment (n = 5-8 mice per group). (D) Liver weight at terminal workup (n = 5-8 mice per group). (E) Time course of blood counts and GFP-chimerism of recipient mice (n = 6-8 mice per group). (F) Frequencies and GFP-chimerism of hematopoietic stem cells (LT-HSCs) in bone marrow and spleen at terminal workup after 12 weeks of treatment (n=5-8 mice per group). Two-way analysis of variance (ANOVAs) with subsequent Tukey posttest was used. \*P < .05, \*\*P < .01, \*\*\*P < .001, \*\*\*\*P < .0001.

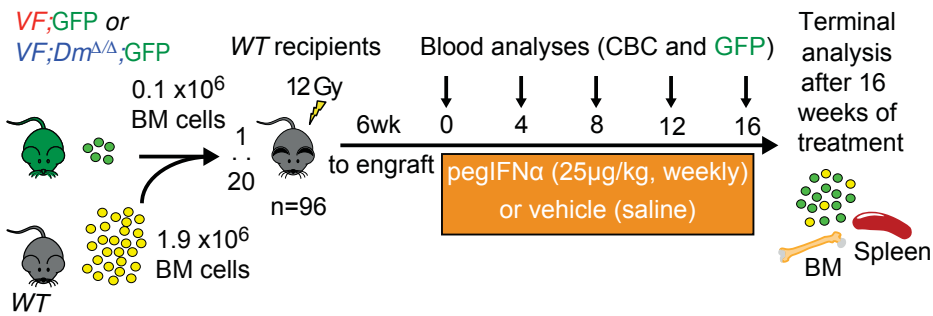
# Figure 1



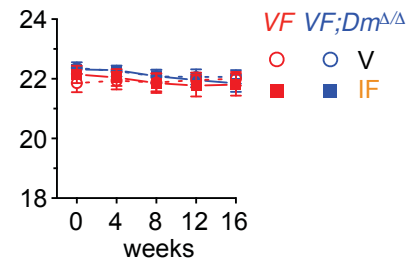
Downloaded from <http://aspubs.cup.com/doi/10.1182/blood.2023020270/2218293/blood.2023020270.pdf> by guest on 06 May 2024

## Figure 2

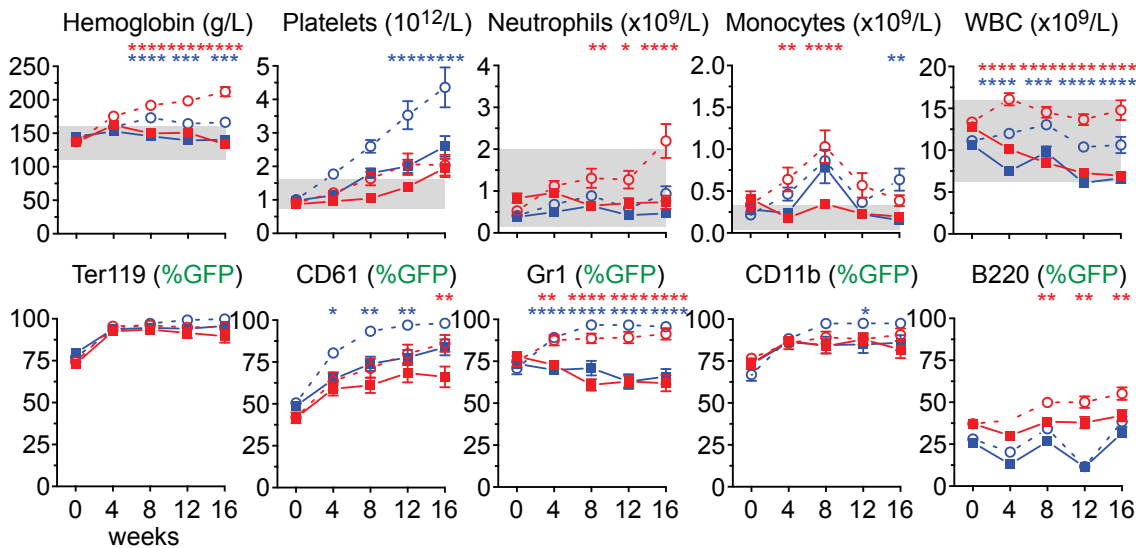
### A Timeline of competitive 1:20 transplantations and treatment with peg-IFN $\alpha$



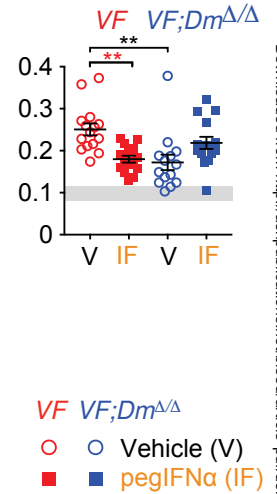
### B Body weight (g)



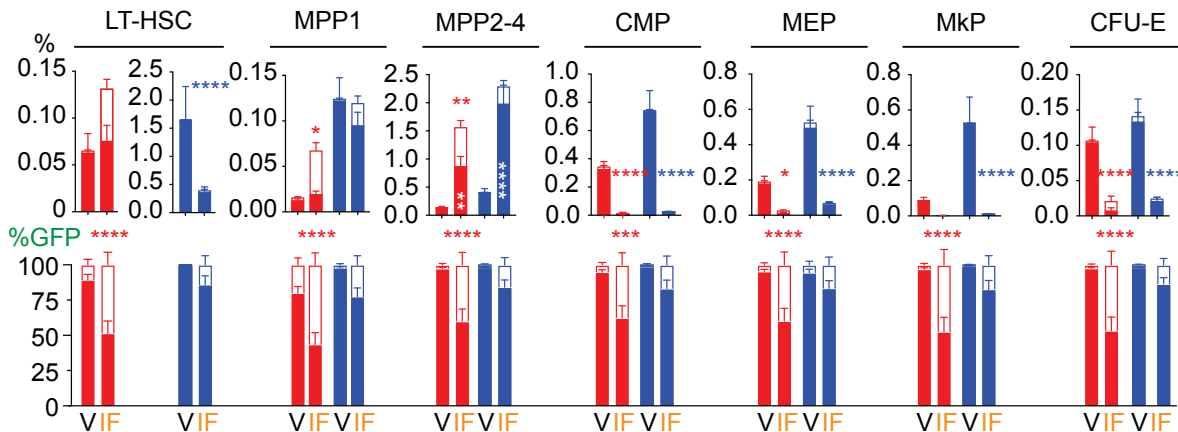
### C Blood counts and GFP chimerism



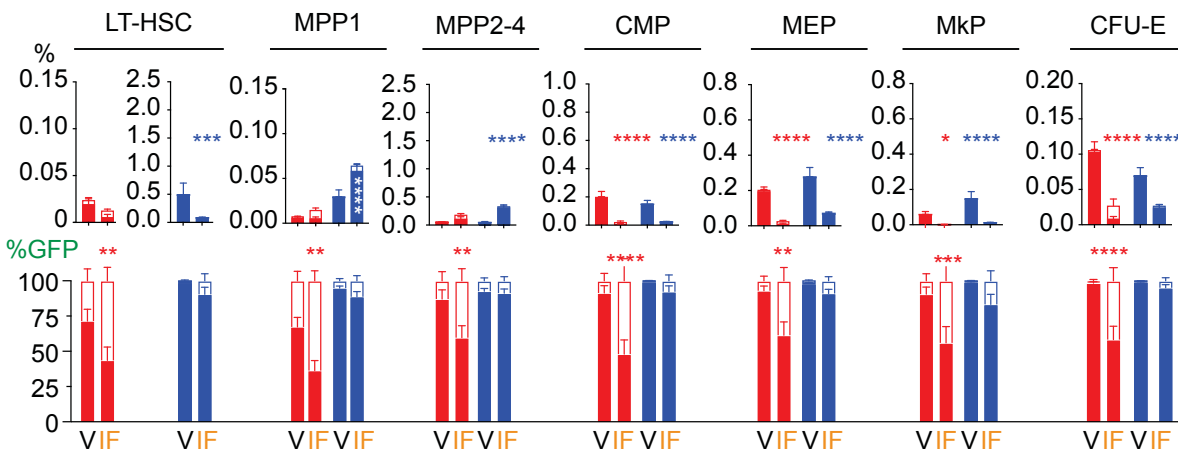
### D Spleen weight (g)



### E Frequency and GFP chimerism in HSPCs cells from bone marrow



### F Frequency and GFP chimerism in HSPCs cells from spleen



### G % of CD41<sup>hi/lo</sup> cells within GFP<sup>+</sup> LT-HSCs

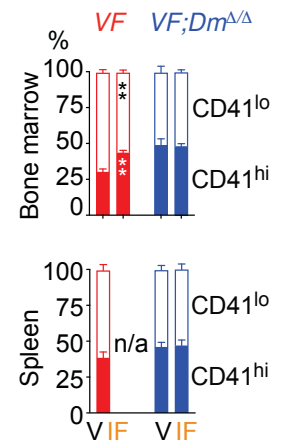
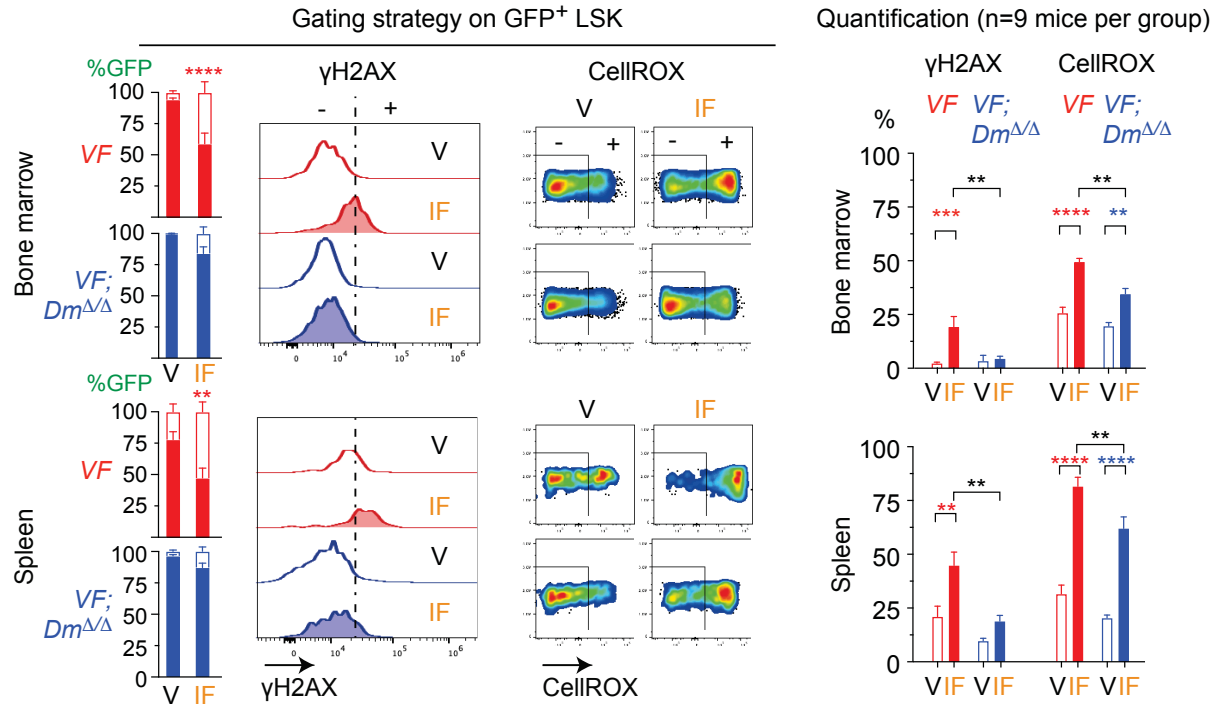
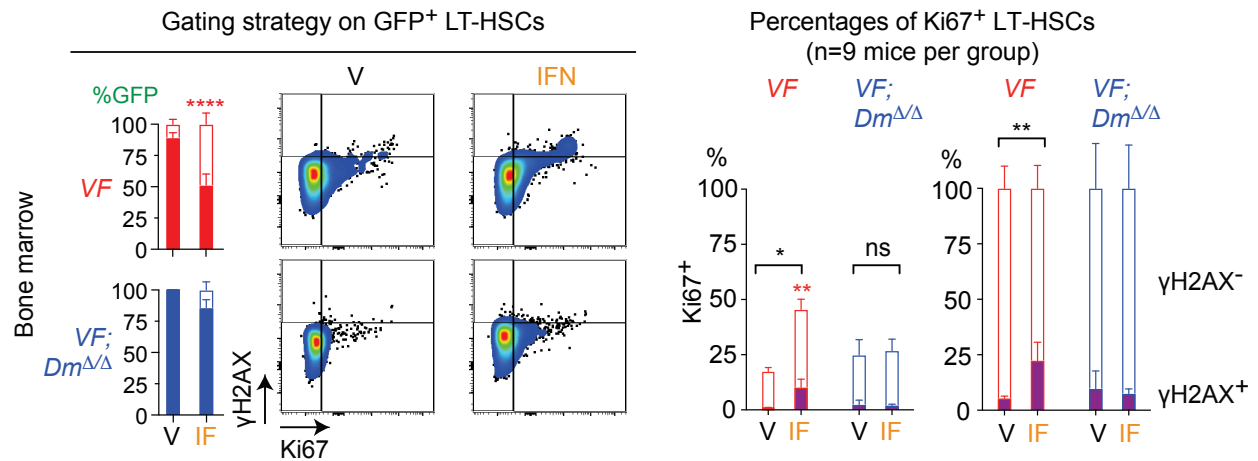


### Figure 3

#### A Analysis of DNA damage and ROS accumulation in GFP<sup>+</sup> LSK cells



#### B Analysis of cell division and DNA damage within the GFP<sup>+</sup> LT-HSCs



#### C ROS accumulation in GFP<sup>+</sup> LT-HSCs (n=8 mice per group)

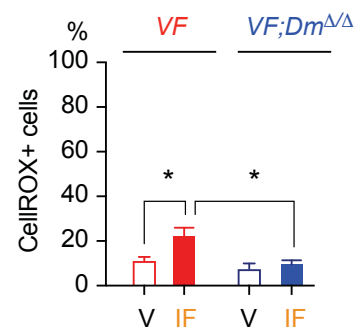
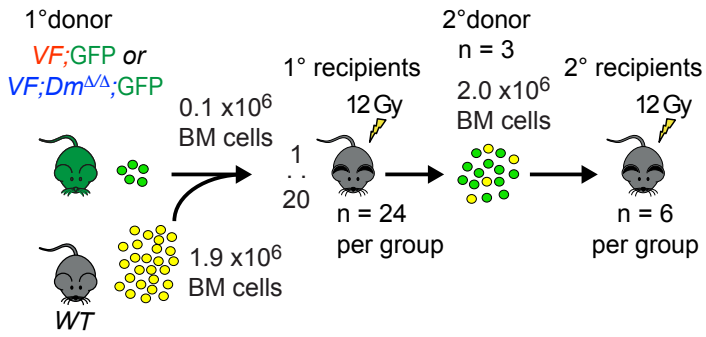


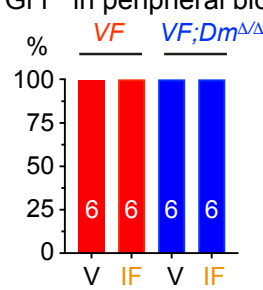


# Figure 4

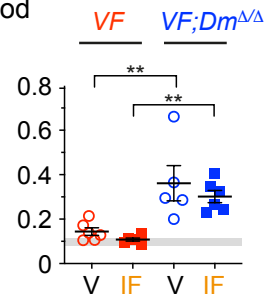
## A Non-competitive transplantations into secondary hosts



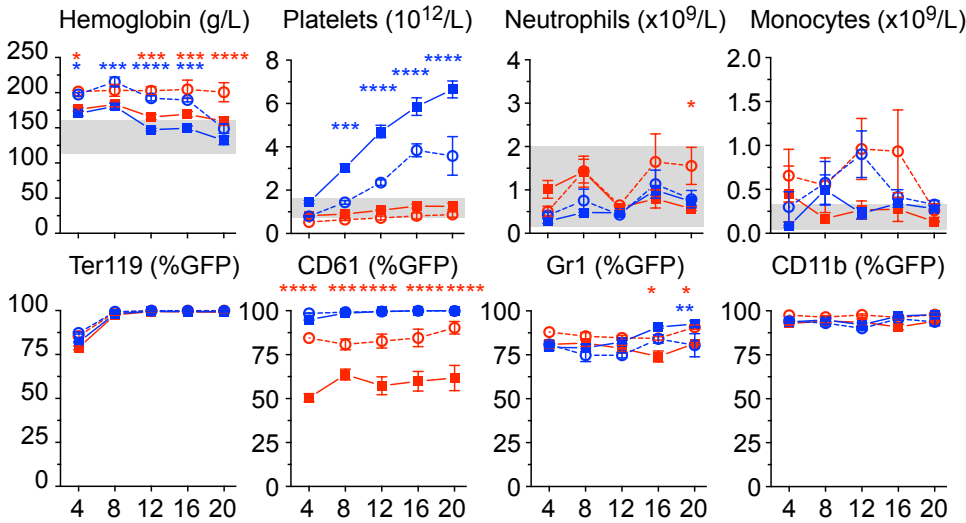
## B Mice with >1% GFP<sup>+</sup> in peripheral blood



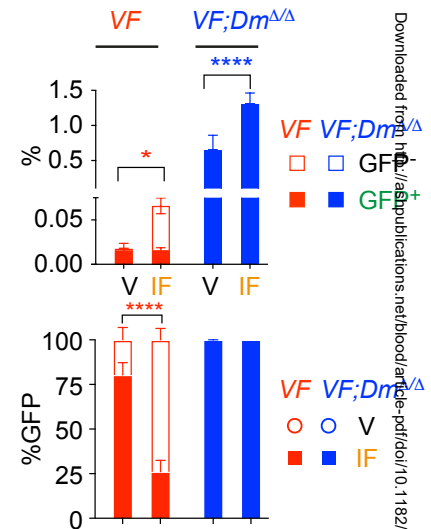
## C Spleen weight (g)



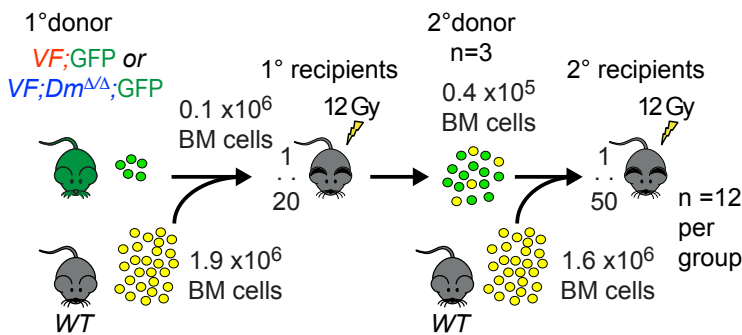
## D Blood counts and GFP chimerism in secondary non-competitive recipients



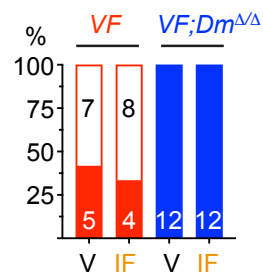
## E LT-HSCs in bone marrow



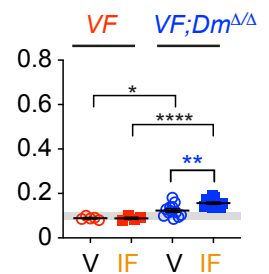
## F Competitive 1:50 transplantations into secondary hosts



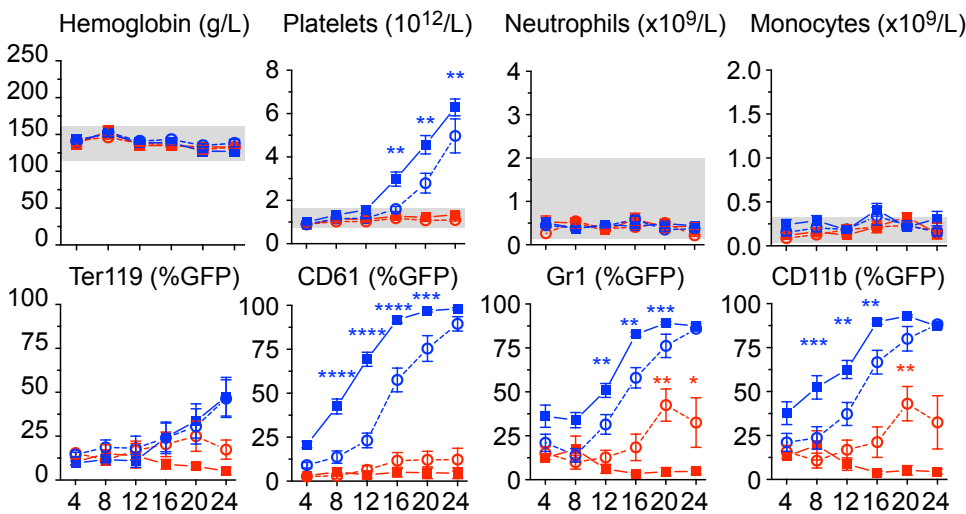
## G Mice with >1% GFP<sup>+</sup> in peripheral blood



## H Spleen weight (g)



## I Blood counts and GFP chimerism in secondary 1:50 recipients



## J LT-HSCs in bone marrow

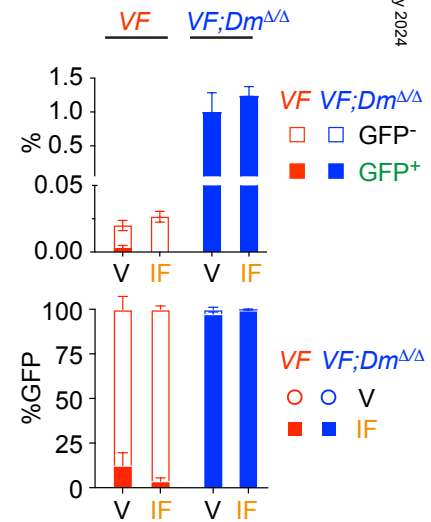
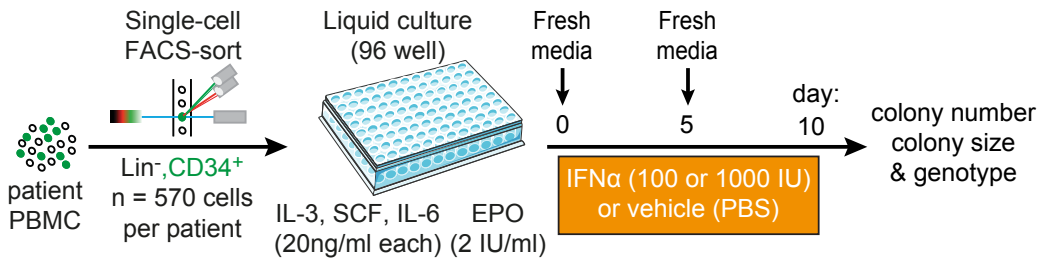
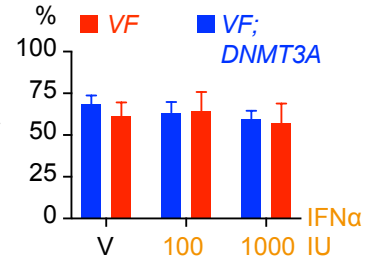


**Figure 5**

**A** *Ex-vivo* IFN $\alpha$  treatment of human HSPCs from MPN patients



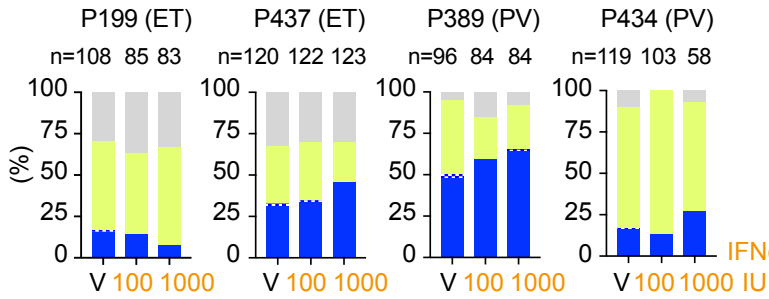
**B** Efficiency of colony growth



**C** Genotyping of HSPC-derived colonies treated with IFN $\alpha$  or vehicle

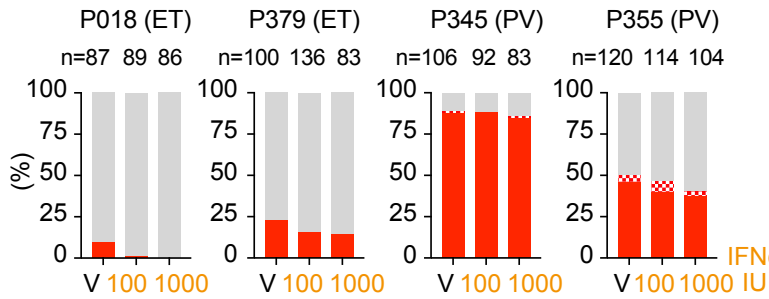
Patients with *JAK2-V617F* and *DNMT3A* mutations

<i>DNMT3A</i>	<i>JAK2</i>
WT	WT
het	WT
het	VF hom
het	VF het

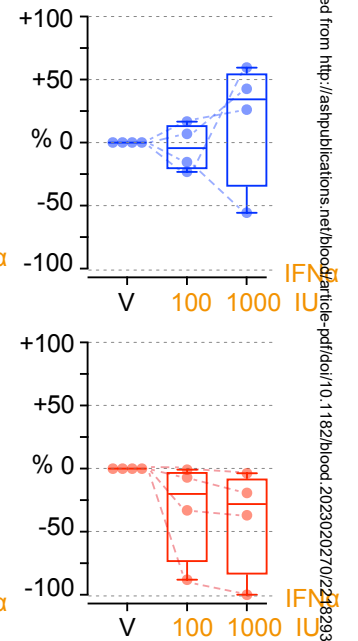


Patients with *JAK2-V617F* mutation only

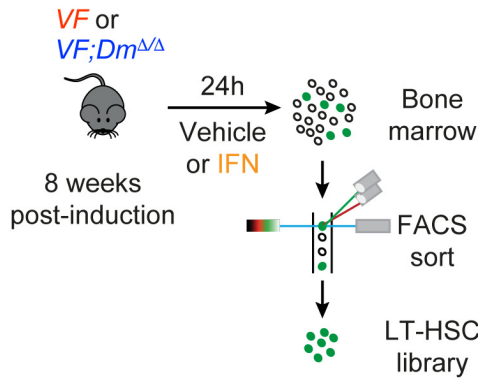
<i>DNMT3A</i>	<i>JAK2</i>
WT	WT
WT	VF hom
WT	VF het



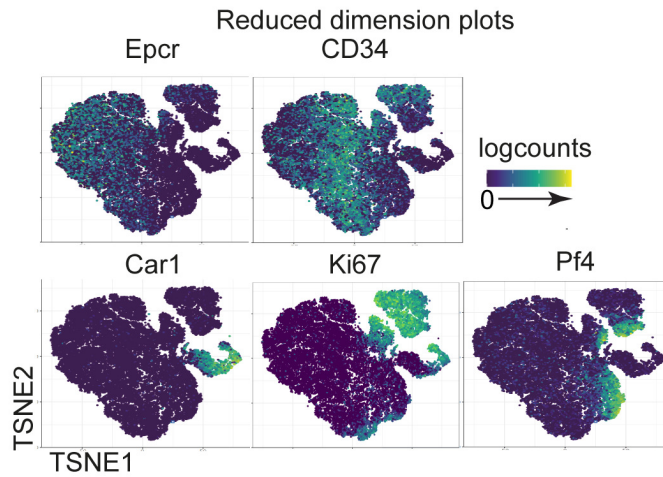
**D** Relative change (%) in *JAK2-V617F*<sup>+</sup> colonies



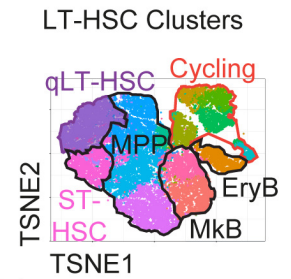
### A Setup of IFN $\alpha$ treatment and sorting



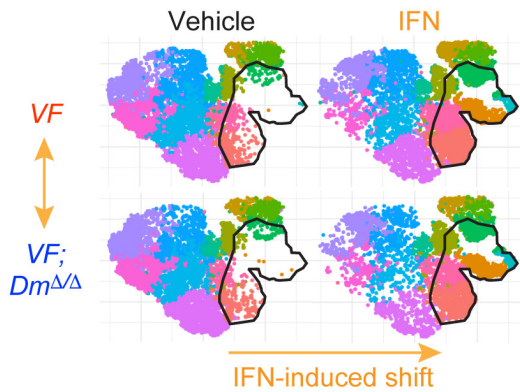
### B Clustering analysis of sorted LT-HSCs



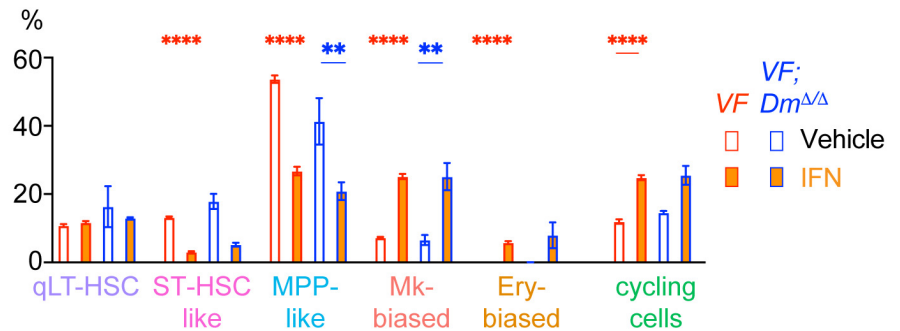
### C Cell identity



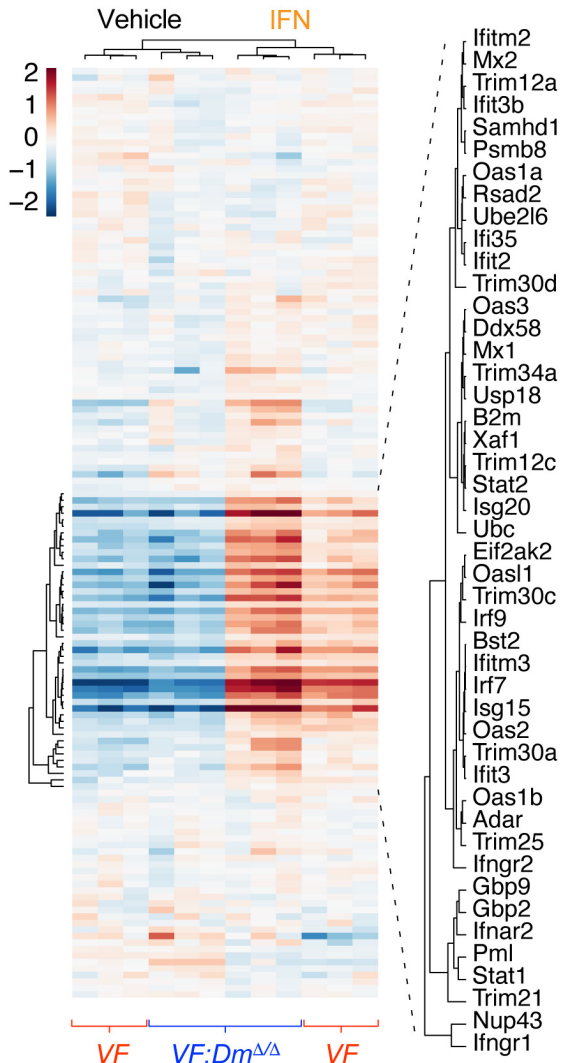
### D Shift in cell identity in sorted LT-HSCs induced by IFN $\alpha$ treatment



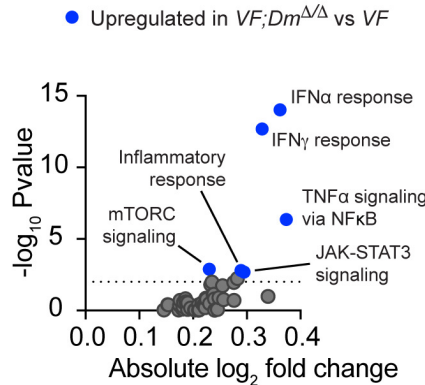
### Quantification of LT-HSC subclusters within sorted LT-HSCs



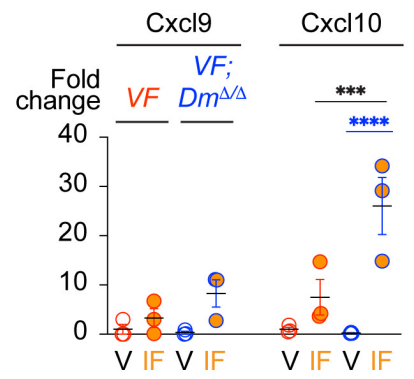
### E IFN-response genes in qLT-HSC



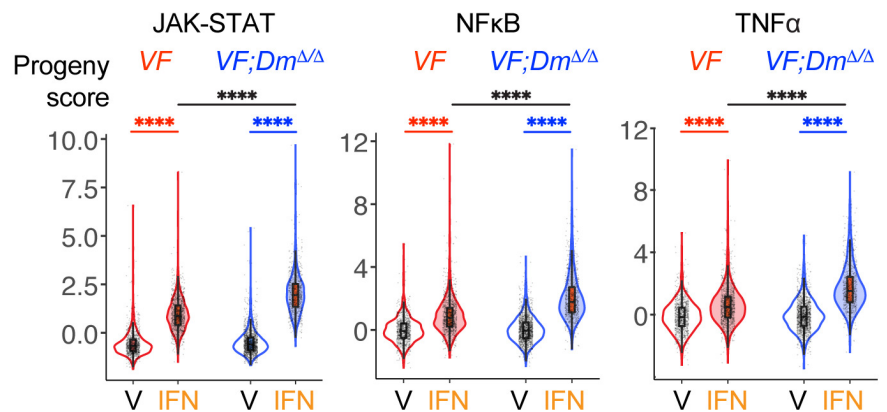
### F GSEA analysis in qLT-HSCs treated with IFN (Hallmark)

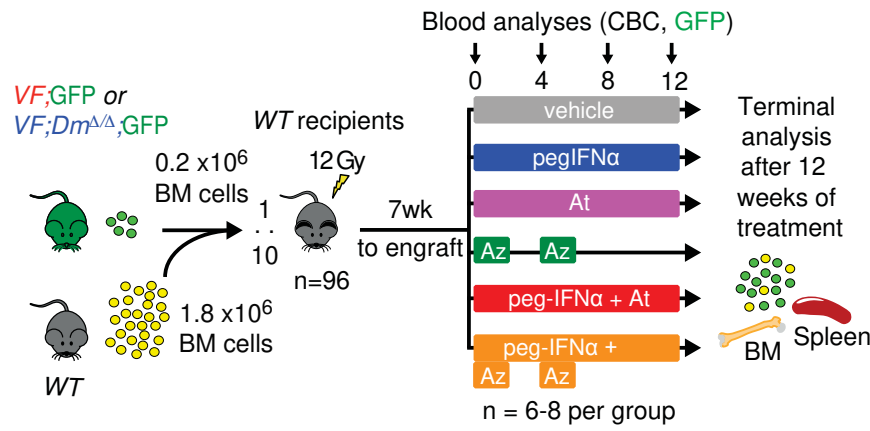
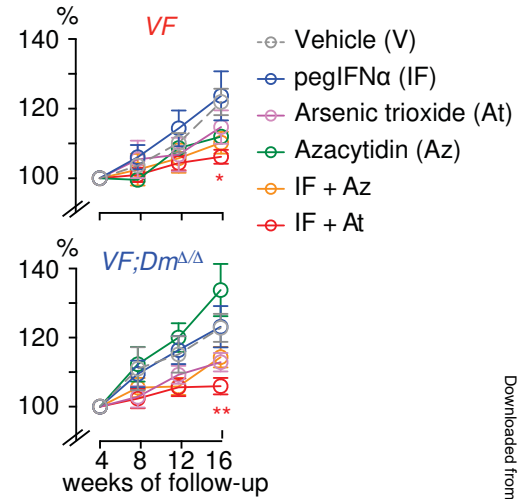
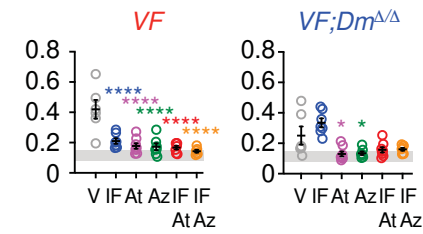
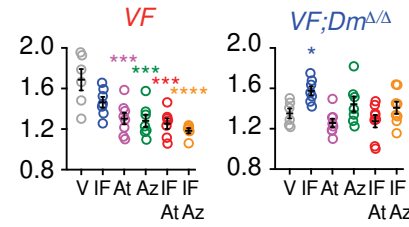
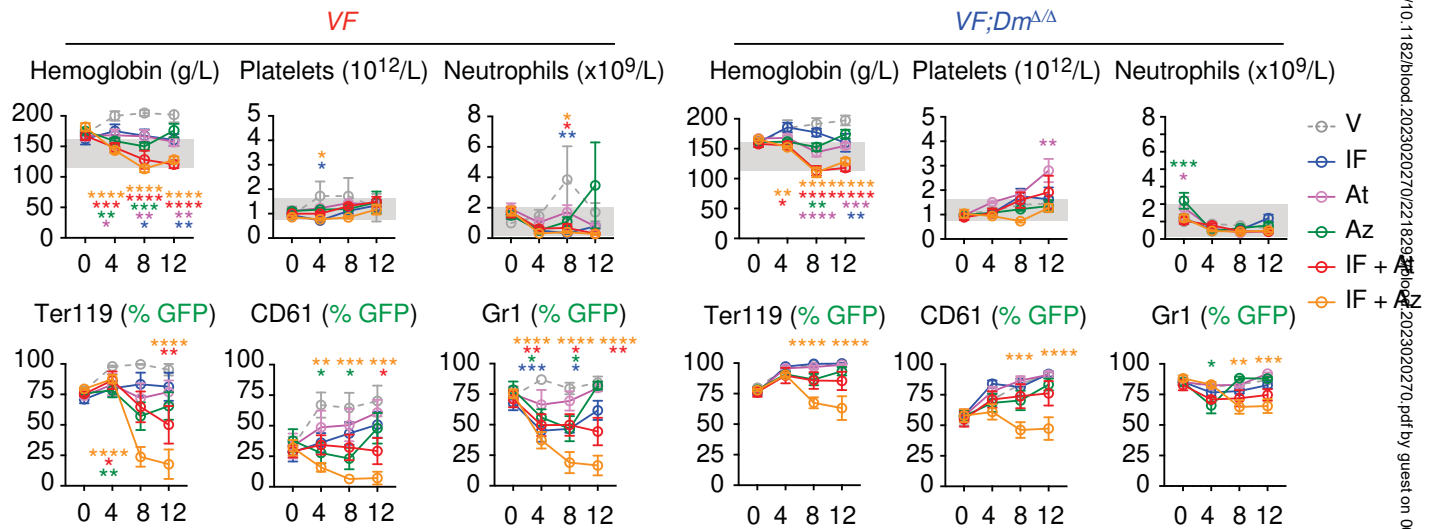
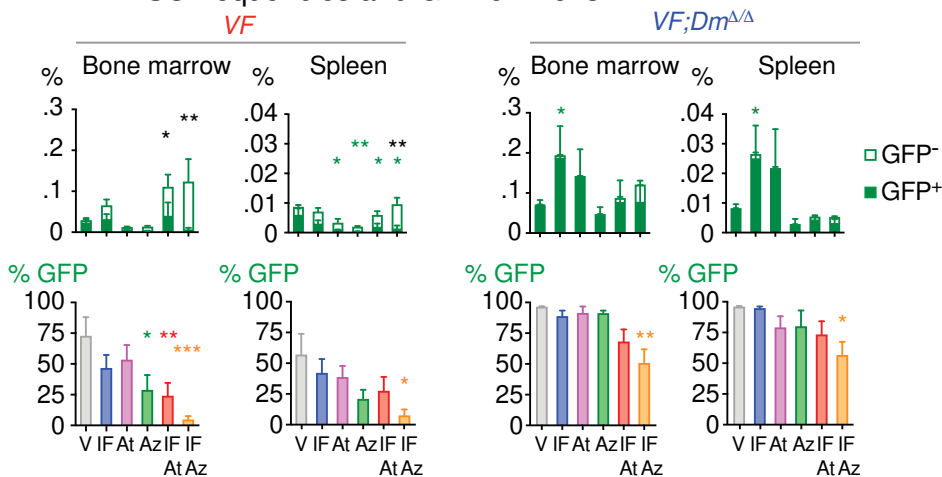


### G INF-inducible chemokines in quiescent LT-HSC

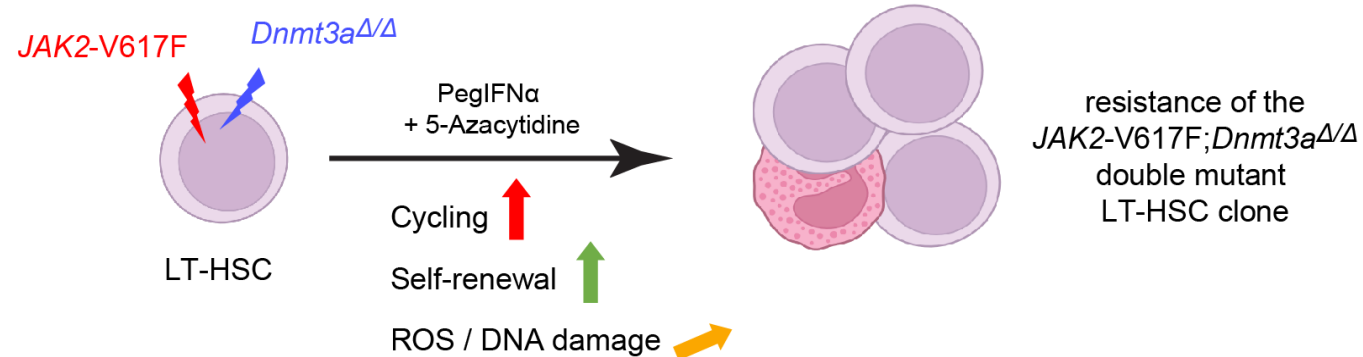
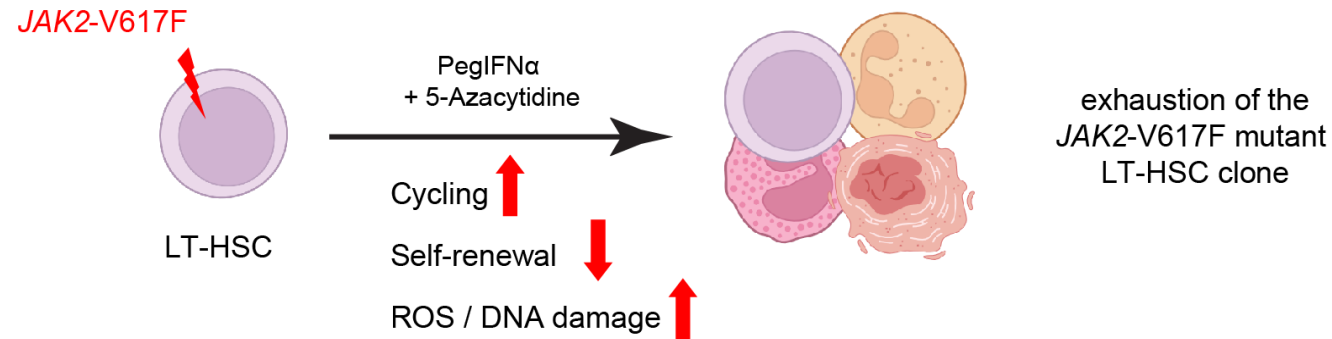


### H Progeny analysis in quiescent LT-HSC



**Figure 7****A Schematic drawing of the experimental setup****B Body weight (% of change)****C Spleen weight (g)****D Liver weight (g)****E Time course of blood counts and GFP chimerism****F LT-HSC frequencies and GFP chimerism**

## Effects of *Dnmt3a* deletion in *JAK2*<sup>V617F</sup> MPN on responses to treatment with pegIFN $\alpha$ and 5-azacytidine



- The combination of pegIFN $\alpha$  and 5-azacytidine strongly depletes *JAK2*-V617F mutant hematopoietic stem cells.
- Loss of *Dnmt3a* increases self-renewal of *JAK2*-V617F mutant hematopoietic stem cells and mitigates their attrition by pegIFN $\alpha$  alone or the combination with 5-azacytidine.